EVAPOTRANSPIRATION OF GROUNDWATER: A TIME SERIES ANALYSIS OF THE HYDROLOGIC REGIMEN OF A GROUNDWATER DISCHARGE AREA

by

RICHARD E. JACKSON

Submitted in partial fulfillment
of the requirements for the degree of
Master of Applied Science

Department of Civil Engineering
School of Graduate Studies
University of Ottawa
Ottawa, Canada

December 1971

History is neither determined or random. At any moment it moves forward into an area whose general shape is known but whose boundaries are uncertain in a calculable way.

Jacob Bronowski, The Common Sense of Science

ABSTRACT

Methods of time series analysis have been employed to examine climatological and hydrogeological variables associated with a groundwater discharge area at Delta, Manitoba.

Nonrandom components associated with the weather and circulation of the North American summer climate were identified in both the climatological and hydrogeological variables.

The hydrogeological variables, daily groundwater evapotranspiration and daily groundwater inflow rate, were satisfactorily described by first-order Markov processes.

Statistical filtering of the hydrogeological variables showed that two hydrogeological processes were associated with seasonal maxima in the daily groundwater evapotranspiration time series. Both occurred in the presence of hot weather and a shallow water table. One process was associated with strong upward groundwater flow to the water table in the discharge area due to the propagation of recharge through the flow system, while the other was due to infiltration and the Lisse effect causing a rise in the water table in the discharge area.

Results from the study explain why the water table fluctuates within a small range of depth in a groundwater discharge area, a major assumption of the steady-state, mathematical model of groundwater flow systems.

ACKNOWLEDGEMENTS

This research project was carried out under the auspices of the Career Introductory Program of the Groundwater Subdivision, Hydrologic Sciences Division, Inland Waters Branch. The author is much indebted to the members of the Subdivision, especially to J. A. Gilliland who supervised the author's work.

The author is similarly indebted to Dr. K. Adamowski, of the University of Ottawa, who supervised his academic work and encouraged the author to seek more physically-oriented uses of time series analysis and to Dr. F. P. Agterberg, of the Geological Survey of Canada, who advised the author on the method of filtering and very kindly made available his computer program.

No results would have been possible without the field data. Bob Weaver of the Instrumentation Section, Hydrologic Sciences Division, installed the instruments at Delta, and Bill Carmichael, of Portage la Prairie, changed their charts. The author is deeply grateful to both.

While at the University of Ottawa the author's research was supported by a bursary from the National Research Council of Canada.

TABLE OF CONTENTS

LIST OF FIGURES

NOTATIONS

Major Abbreviations

acf = autocorrelation function

acvf = autocovariance function

Var = variance

Greek Symbols

α = confidence level probability

ε = limiting value of error in the corrected filter

μ = mean

ξ = some point on a real line

$\rho(\ell)$ = theoretical acf

ΣH = sum of filter values

Δs = daily drawdown of hydrograph

$\chi^2_{T_m}(\alpha)$ = chi-square value

ℓ = lag

Other Symbols

a = fitted acf coefficient

$B(\ell)$ = theoretical acvf

$b(\ell)$ = the filter

$b'(\ell)$ = the corrected filter

c = fitted acf coefficient

$C(\ell)$ = estimated acvf

$C^*(\ell)$ = modified apparent acvf

$D(\ell)$ = lag window

$E|\ |$ = expected value

$F|\ |$ = distribution function

$G(\ell)$ = smoothed estimate of spectral density

$g(\ )$ = function of

H = cumulative distribution function of variance

H' = probability density function of variance

$h(\ell)$ = theoretical spectral density

$K(s,t)$ = covariance kernal

m = lag

n = sample size

$N(k)$ = noise (population)

$n(k)$ = noise (sample)

P = probability

$\overline{P}$ = daily precipitation in inches

p = filter coefficient

q = filter coefficient

Q = groundwater evapotranspiration in feet/day

r_k^* = acf significance test coefficient

R_k = coefficient in chi-square test

$R(\ell)$ = estimated acf

R = groundwater inflow rate in feet/hour

r_1 = lag one acf coefficient

$S(k)$ = signal (population)

$s(k)$ = signal (sample)

S_y = specific yield

t = time

T = set containing all possible t

$\overline{T}$ = mean daily temperature in degrees Fahrenheit

T_m = maximum lag

t_p = student's variable at probability level p

$V(\ell)$ = raw estimate of spectral density

v, v' = degrees of freedom

$X(t)$ = random variable or stochastic process (population)

$x(t)$ = sample of $X(t)$

TIME SERIES

$\overline{P}(t)$ time series of $\overline{P}$

$Q(t)$ time series of Q

$R(t)$ time series of R

$\overline{T}(t)$ time series of $\overline{T}$

CHAPTER 1

INTRODUCTION

1.1 Motivation

The development of the high-speed, digital computer in the 1950's led to spectacular advances in hydrology in the following decade. Appropriately enough some of these advances were made at the beginning of the International Hydrological Decade (I.H.D.) of 1965-1975, whose purpose was to enable all countries to make a fuller assessment of their water resources and a more rational use of these resources by industry, agriculture, and the populace in general. Fundamental to these purposes was the intention of the I.H.D. to promote research and education in scientific hydrology.

Among the areas that were identified as being not only in the spirit of the I.H.D. but also in need of urgent attention by Canadian hydrologists was that of the "correlation of groundwater observations with meteorological parameters" (8). The atmosphere is the source of recharge to the groundwater reservoir and the sink for discharge of evapotranspiration of groundwater. Fortunately the advances of the 1960's produced mathematical methods and hydrologic models with which to analyse the groundwater-climate regimen.

Geophysicists in general, and hydrologists in particular, have gained much information from their data by

using a family of mathematical methods collectively called time series analysis. In hydrology these methods have produced more reliable predictions of upper bounds for streamflow discharges, techniques for identifying nonrandom components in a data sequence, and an approach for examining the relationship between variables (20).

Perhaps the most impressive advance in conceptual hydrologic modelling since the work of Perrault, Mariotte and Halley in the seventeenth century has been that of the dynamic, groundwater flow system. Meyboom's (29) Prairie Profile (Figure 1, p.3) is the classic case of a regional, groundwater flow system and his words suffice to define it.

> "By definition the Prairie Profile consists of a central topographic high bounded at either side by an area of lower elevation. Geologically the profile is made up of two layers of different permeability, the upper layer having the lower permeability. Through the profile is a steady flow of groundwater from the area of recharge to the area of discharge. The ratio of permeabilities is such that groundwater flow is essentially downward through the material of low permeability and lateral and upward through the underlying more permeable layer."

Freeze (14), in developing a steady-state, mathematical model of the regional groundwater flow system,

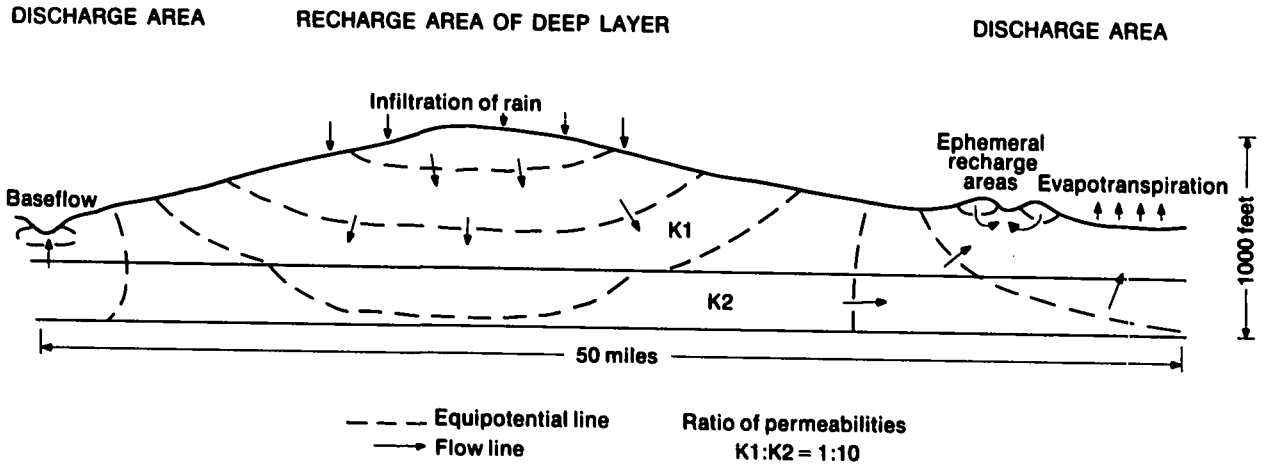

FIGURE 1.1 MODIFIED PRAIRIE PROFILE

introduced the concept of the dynamic equilibrium:

> "The recharge to the water table (or the discharge from the water table) is the amount necessary to maintain it in its equilibrium position at every point along its length at all times. It is thus a case of dynamic equilibrium. This assumption of a steady water table enables us to treat regional groundwater flow as a steady-state problem."

The discharge to which Freeze refers generally takes two forms -- baseflow and evapotranspiration.

The motivation of this study was to explore the potential of using the mathematical methods of time series analysis and the conceptual model of the groundwater flow system in analysing the groundwater-climate regimen. It is the objective of this study to employ time series analysis to examine the climatological and hydrogeological variables associated with the evapotranspiration from a groundwater discharge area.

1.2 Literature Review of the Groundwater-Climate Regimen

It is necessary to first define a few fundamental terms. The water table is that imaginary surface beneath the ground at which the pressure is atmospheric. The saturated zone above the water table, the capillary fringe, is at a pressure less than atmospheric, consequently the water table must be defined on the basis of pressure rather than water content. "A dis-

charge area is an area where the direction of groundwater flow is toward the water table" (14), whereas in the recharge area the direction of flow is away from or parallel to the water table. Therefore recharge is that flow whose vertical component is downward, and discharge is that flow whose vertical component is upward.

Meyboom (30) ascribed the natural fluctuation of water-table levels on the Canadian Prairies to rain, barometric pressure, temperature and evapotranspiration. Each is a part of the groundwater-climate regimen.

1.2.1 The Effects of Rain

In soils in which the water table lies within 3 feet of the surface, it has been frequently observed that a light rain will cause an immediate and disproportionate rise of the level in an adjacent well. This phenomena, which is not due to recharge by infiltration, is known as the Lisse Effect. Commonly an inch of infiltrated rain will cause an 18 inch rise of the water table. Meyboom (30) reported that this phenomenom is caused by the following process:

> "Rain infiltrating evenly into the light soil acts as a tight closing lid compressing the air above the capillary fringe. If "n" is the depth of the rain penetration and "h" the distance from the surface to the top of the capillary fringe, the pressure increase of the air above the capillary

fringe is given by Hoogboudt as:

$$\frac{h}{h-n} - 1 = \frac{n}{h-n} \text{ atmospheres} = \frac{n}{h-n} \times 35 \text{ feet of water."}$$

The re-establishment of equilibrium of the soil-moisture system necessitates a rise in the phreatic surface of n/(h-n) x 35 feet of water. Figure 1.2, p.7 shows an example of the Lisse Effect, where a 0.22 inch rainfall produced a rise of 0.31 feet in the well giving a rain-to-rise ratio of 1:17.

Meyboom (30) in quoting a Dutch report by Hooghoudt has noted that another process, the Weiringermeer Effect, may also cause anomalies appearing on groundwater hydrographs. In those cases in which the capillary fringe is close to the surface, rain produces an almost instantaneous rise in the hydrograph followed by an equally fast decline due to evaporation.

1.2.2 The Effect of Barometric Pressure

It has been only in the last decade that hydrologists have investigated the effect of changing barometric pressure on an unconfined aquifer. Peck (33) discussed the effects of entrapped air on the water table when the aquifer is subjected to changing barometric loads. Meyboom (30) pointed out that a thunderstorm would produce the opposite effect as would the Lisse Effect, that is a rise in the hydrograph due to reduced atmospheric pressure. Gilliland (15) developed a general

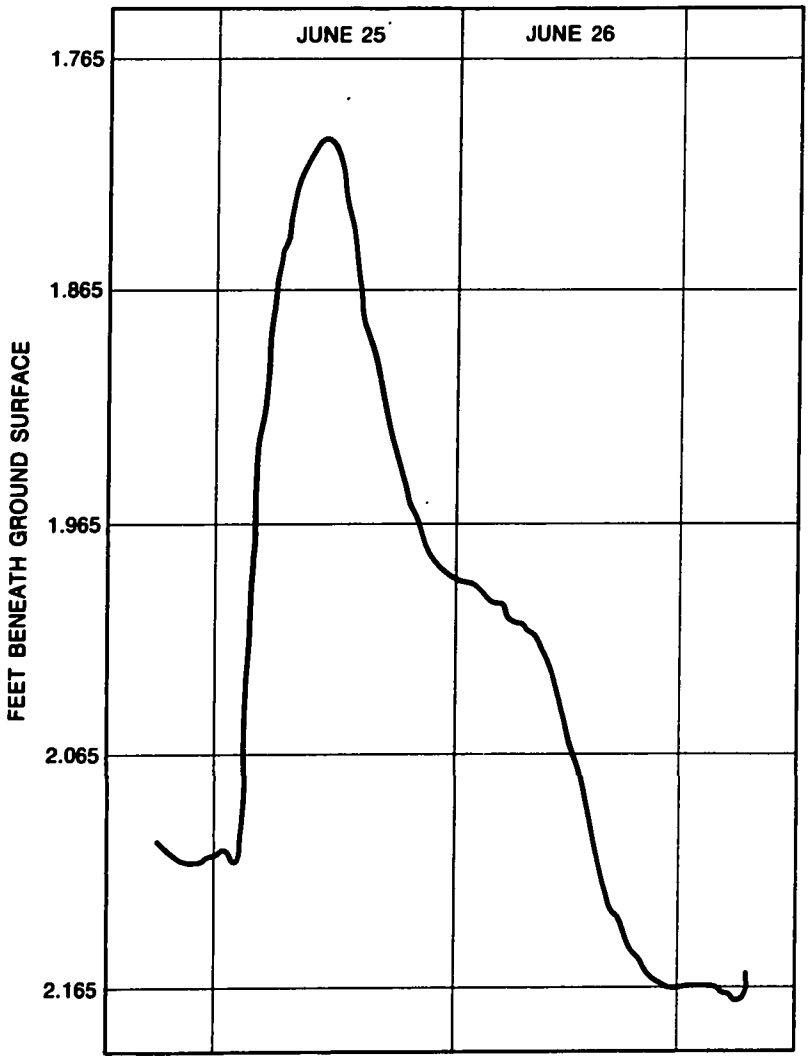

FIGURE 1.2 LISSE EFFECT AT D-1
DUE TO 0.22 INCHES OF RAIN

theory, the rigid plate model, to explain the effects of barometric pressure on confined and unconfined aquifers. The model relates the barometric efficiency of the aquifer, that is the slope of the regression of the hydrograph on the barograph, to the hydrology of the aquifer and the soil moisture zone, which acts as a rigid plate modifying the effects of changing barometric loads on the aquifer.

Let it suffice to say that generally the water table responds inversely to the barometric pressure due to air pockets within the saturated zone.

1.2.3 The Effects of Temperature

If only the direct effects of air temperature on unconfined aquifers are considered there are two processes which can produce diurnal fluctuations of the water table.

In the first case the diurnal fluctuation is due to the physics of the capillary fringe. Capillary rise is directly proportional to the interfacial tension between water and soil particle which, in turn, is inversely proportional to the temperature of the soil. When the capillary fringe is sufficiently close to the surface to be affected by the diurnal fluctuation of soil temperature, that is within the upper 20 cm of the soil horizon, the increased daytime soil temperature causes a decrease in the interfacial tension and a subsequent dewatering of the capillary fringe, which, in turn, causes a diurnal rise of the water table.

The second process, that of water vapour transfer along a temperature gradient, could produce a diurnal fluctuation if the gradient was reversed by the diurnal air temperature fluctuation. In this case the vapour flow would be downward during the day from the surface to the capillary fringe, and upward at night.

Meyboom (30) concluded from his Saskatchewan study that the effect of temperature on the interfacial tension was not observable during the summer since the capillary fringe was too deep and the diurnal evapotranspiration signal was too dominant. By October the situation had changed with the autumnal rains raising the water table and the first frosts killing the vegetation, hence halting the summer drawdown due to evapotranspiration. During the autumn Meyboom observed several days with diurnal fluctuations having a peak in the late evening, indicating the presence of one or both of the above-mentioned processes.

1.2.4 The Effect of Evapotranspiration by Phreatophytes

Meinzer (27) defined the phreatophyte as a plant "that habitually obtains its water supply from the zone of saturation, either directly or through the capillary fringe." Meyboom (28) has noted that while Meinzer's statement applies to the semi-arid Canadian Prairies, "where abundant soil moisture is normally lacking", most species can survive in

moist unsaturated environments. In fact Jaworski (18) has implied that in more humid areas, at least, the unsaturated zone is the more fundamental source.

White (42), in his classic study of phreatophytes in the Escalante Valley, Utah, credited Professor Smith of the University of Arizona with being the discoverer of the cause of the diurnal fluctuation of shallow water tables in areas of vigorous growth of cottonwood and mesquite. In 1922 Smith delivered an unpublished address to the Geological Society of Washington explaining that the decline of the water table during the afternoon and its subsequent rise at night and during the following morning (Figure 1.3, p.11) was, in White's words, "due to withdrawal of groundwater from the zone of saturation by the trees."

It is now known that the recovery at night is due to natural groundwater discharge; in Meyboom's (30) word's, "phreatophytes live by virtue of the nightly recovery of the water table."

Meyboom (30) described evapotranspiration as a "'necessary evil' related to the gas exchange, which is required for photosynthesis and respiration." It is also vital in the heat regulation and ion transport within the plant. Water evaporating from a leaf causes the sap concentration of the leaf to increase, thereby producing an osmotic gradient between adjacent cells in the plant. This gradient

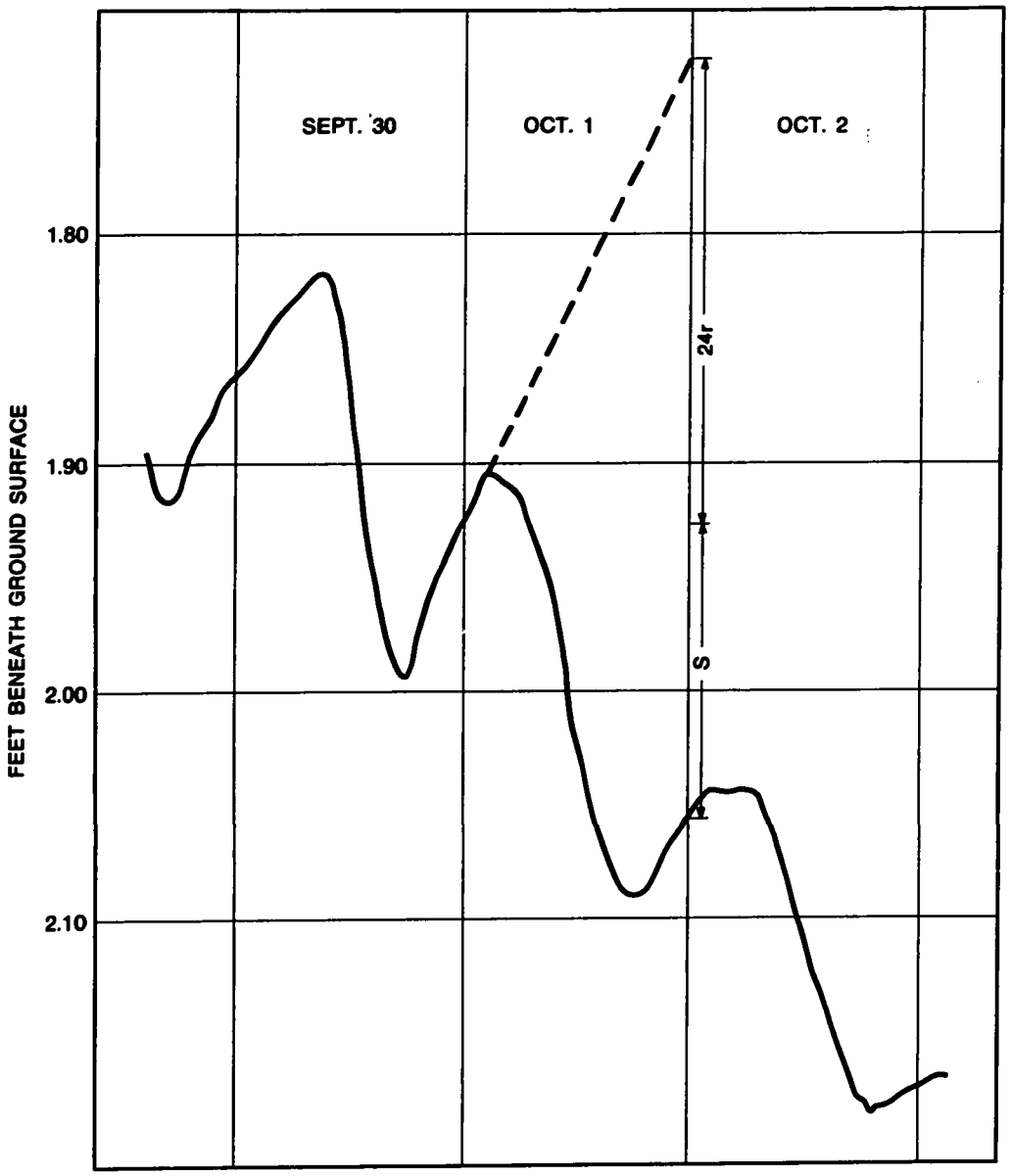

FIGURE 1.3 DIURNAL FLUCTUATIONS DUE TO EVAPOTRANSPIRATION AT K-1

"pumps" the soil moisture and groundwater through the roots, up the xylem to the leaf and then through the stomata, from whose surface it is evaporated.

Numerical methods for computing daily evapotranspiration of groundwater by hydrograph analysis have been proposed by White (42) and Troxell (41). Of the two methods the former is less subjective and more widely known. White estimated daily groundwater evapotranspiration (Q), from the specific yield of the soil in which the fluctuations occur (Sy), the hourly groundwater inflow rate (R), and the daily change in water level due to evapotranspiration (Δs):

$$Q = Sy(24R + \Delta s) \qquad 1.1$$

It should be noted that R refers not to infiltration but to subsurface discharge due to the fact that these fluctuations occur in groundwater discharge areas where the flow lines of the regional groundwater flow system converge towards the surface. R is measured (Figure 1.3, p.11) by taking the slope with respect to time of the hydrograph during the night. A negative value of R indicates that the water table is draining, while a positive value indicates subsurface discharge.

The works of White (42), Robinson (38), McDonald and Hughes (25), and Meyboom (30) have pointed to the intimate relationships between air temperature and the depth to the water table on phreatophytically-induced groundwater fluctuations.

Meyboom (30), by comparing evapotranspiration in a greenhouse with that of an open, adjacent site in the same wolf willow patch, showed that an 8°F rise in temperature and a 30% increase in the relative humidity due to the greenhouse environment doubled the evapotranspiration of groundwater. This experiment concisely demonstrates the dominant effect of temperature since "the effect of the relatively slight rise in temperature is far greater than the opposite effect of the rise in relative humidity" (30).

McDonald and Hughes'(25) work at Yuma, Arizona has raised some interesting points about the relationship between air temperature, solar radiation and evapotranspiration. They observed that their hydrographs changed from a falling to a rising stage within 15 minutes of the first rays of the sun striking the area of the well. Furthermore they noted that the maximum shortwave solar radiation occurred in June while the maximum amplitude of the diurnal fluctuations occurs in October, by which time the summer rains from the Gulf of Mexico have brought the water table close to the surface and into the reach of the roots of more phreatophytes. Consequently, allowing that there is a strong relationship between air temperature and solar radiation in arid regions (Sellers (39), 1965), the importance of the temperature-evapotranspiration relationship is modified by the timing of the rainy season and the resulting change in the depth of the water table.

Meyboom (30) stated "that the depth to water is the most important variable governing groundwater consumption, at least in the semi-arid Canadian Prairies". Using simple, linear regression he statistically explained 64% of the variance of the relationship between groundwater consumption of shrubs and herbs and the average depth to the water table. Likewise Robinson ((38) p.18) compiled data from all over Western U.S.A. and graphically demonstrated the importance of the relationship.

1.3 Literature Review of Time Series Analysis

Because of the proliferation of uses of time series analysis it is necessary to define certain fundamental terms. First it is appropriate to use Kendall and Stuart's (21) definition of a time series:

> "Observations on a phenomenon which is moving through time generate an ordered (sequence) known as a time series."

A time series is assumed to be composed of three additive components -- the trend, the periodic component and the random component. The trend is a slow, gradual change of a variable over the period of record. The periodic component "is a fluctuation imposed on the series by a cyclic phenomenon external to the main body of causal influences at work upon it" (21). The random component "evolves, entirely or in part, according to a random mechanism." (22). It should be noted

that any periodic component with a period much longer than the record will appear as a trend and not as a periodic fluctuation.

A deterministic process or variable is defined throughout its entire time of existence by an equation which predicts the process with unit probability. On the other hand a stochastic process develops in time due, wholly or in part, to a random mechanism and can only be predicted with a probability of less than one.

A stationary time series has a mean and variance that are constant in time. This concept is defined more rigorously in Section 2.1.

Persistence is "the existence, at some (time) lag k, of a serial correlation coefficient R(k) which is significantly greater than zero with some level of assurance." (11).

1.3.1 Applications in Hydrogeology

The first workers to consider the groundwater hydrograph as a time series were Remson and Randolph (37). By fitting a least-squares line to the trend component of a hydrograph, they showed how certain aquifer constants could be estimated. Meyboom (28) later used the same method.

A stochastic process can be analysed by two approaches, that of the time domain and that of the frequency domain. Time-domain analysis shows, by the use of correlation

functions, to what extent points on the hydrograph are related to each other in time. Frequency-domain analysis assigns the observed variance of the random component to an infinite number of periodic components with a continuous distribution of frequencies. It is actually a modified form of classical Fourier analysis.

Gilliland (16) was the first hydrogeologist to employ the time-domain methods of time-series analysis. He showed by the use of auto- and cross-correlation functions how to determine whether small fluctuations in ground-water hydrographs are due to barometric or evapotranspiration effects.

Frequency-domain analysis of one variable is more familiarly known as power-spectrum, or, preferably, variance-spectrum analysis. Julian (20), suggested that its use in geohydrology would be in the analysis of "ground-water fluctuations in an effort to study natural regulatory processes." More generally he stated that it can be used for detecting non-random components in a time series and for digital simulation of time series.

The frequency analysis of the covariance of two time series is known as cross-spectrum analysis. From the cross-spectrum and the individual spectra of the two time series one can compute the coherency spectrum, which measures the correlation between the frequencies of the two time series. Julian (20) has suggested the use of the cross-spectrum and

the coherency in those cases which are suited to regression and multivariate analysis.

The application of these spectra to groundwater problems has been pioneered by Eriksson (12,13). Using groundwater levels from a riparian esker, a glaciofluvial deposit, and local air temperature, streamflow and precipitation records, Eriksson found strong persistence in the groundwater, air temperature and streamflow records, but noted that precipitation was almost randomly distributed in time. Furthermore he developed a stochastic model of the water balance of the esker, assuming that the groundwater reservoir was in steady-state, to give estimates of the mean annual infiltration of the esker. Both spectral and coherency analysis showed that at high frequencies wells are more representative of local fluctuations in the water balance than regional ones. This has obvious importance in observation well network design. Complementary to this Eriksson showed that groundwater levels are more sensitive to long-term changes, that is low frequencies, than are river stages.

1.3.2 Application in Climatology

Of those climatic variables which most affect the water balance of a region, precipitation and air temperature are the most important. In examining groundwater hydrographs for non-random components it is necessary to be aware of what non-random periodicities may be contributed by these climatic variables.

Landsberg, Mitchell and Crutcher (23) analysed both short and long records for periodicities in precipitation and temperature. They showed that any six-week record of daily precipitation, regardless of the time of year, had a unique spectrum. That is the spectrum for any particular six-week season varied widely from year to year, with no particular periodicities common to all spectra. However, for several 5-year long records of daily temperature and precipitation, they observed periodicities of approximately 20 days, of 5-7 days, and, for precipitation only, of 3 days. The lesson to be learned here is that it is easier to detect periodic signals when large data samples are used; that is the signal-to-noise ratio increases with record length. The physical importance of the 3-day period was ascribed to a little-understood rapid-pressure wave of this period. However the more familiar 5-7 day periodicity is attributed to the "long waves in the westerlies, first described by Rossby."

Dickson (9) showed that the latitudinal position of major anticyclones over the North American continent was an effective control of the periodicities of mean daily temperature that could be observed at any North American climatic station. If the anticyclone is situated north of the sixtieth parallel it blocks the path of the atmospheric circulation and causes "a southward displacement of the upper westerlies, bringing frequent temperature changes to many U.S. stations" (10). This "high-latitude blocking" is therefore favourable

to short-period oscillations of less than ten days. Dickson also noted that an amplification of the normal summer, upper-level anticyclone over North America favoured periodicities of greater than or equal to 20 days at U.S. stations, while dampening cycles of a shorter period by deflecting the westerlies northward. "Such a pattern has long been recognized as being both a very persistent summer pattern and one associated with drought conditions in the nation's interior" (9).

1.4 Objectives

The objectives of this study are to use time series analysis to: (1) identify, by correlogram analysis, nonrandom components in the climatic variables affecting the groundwater flow system and in the hydrogeological variables associated with evapotranspiration from the flow system; (2) seek a stochastic model of the Markov type to describe these hydrogeological variables; (3) develop a statistical filter to extract the hydrogeological signals from the attendant noise.

CHAPTER 2

MATHEMATICAL METHODS

In order to identify nonrandom components in a time series it is necessary to compute the sample autocorrelation and/or spectral density functions of that time series. Here the sample autocorrelation function is also the basis for the development of the stochastic model and the statistical filter.

2.1 The Nature of Stochastic Processes

Let T be some arbitrary infinite set and let X(t) be some function on T. In mathematical terms therefore $\{X(t) : t \varepsilon T\}$ is a random or stochastic process "in which the set T is the region of time over which the process is defined and the time parameter t belongs to T, the index set of all possible values" (22).

If the sample values $x(t_1)$, $x(t)_2$ .....$x(t_n)$ of the stochastic process from the populations $X(t_1)$, $X(t_2)...X(t_n)$ are statistically independent of one another, the sequence is described as pure random. However if the sequence is internally dependent, that is, serially correlated, then it is described as nonpure random or stochastically dependent. As Kisiel (22) has suggested "we note a spectrum of different processes is possible in nature, ranging from a pure deterministic process to a pure random process."

If $F|x(t)|$ is defined as the distribution function of $X(t)$, that is

$$F|x(t)| = P\{X(t)<x(t)\} \qquad 2.1$$

then the joint distribution function of a n-dimensional random variable may be defined as

$$F|x(1),x(2),\ldots x(n)| = P\{X(t_1)<x(1),X(t_2)<x(2),\ldots X(t_n)<x(n)\} \qquad 2.2$$

The left hand side of Eqn. 2.1 expresses the probability that $X(t)$ takes on a value less than or equal to $x(t)$.

If $F(x)$ is a function defined on an interval (a,b) of a real line, and if (a,b) is divided up into n equal intervals such that $a = x_0 < x_1 < \ldots < x_n = b$, where $\Delta x = x_j - x_{j-1}$ for $j = 1, \ldots n$ then the Stieljes integral with respect to $F(x)$ of a function $g(x)$, as x varies from a to b, is defined as

$$\int_a^b g(x)\, dF(x)$$

which in discrete terms may be written

$$\lim_{\Delta x \to 0} \sum_{i=1}^{n} g(\xi_i)|F(x_i) - F(x_{i-1})|$$

where ξ_i is a point on (a,b) such that $x_{i-1}<\Sigma_i<x_i$.

From the Stieljes integral the expected value or mean is defined as

$$E|X(t)| = \mu_t = \int_{-\infty}^{-\infty} x(t)\, dF|x(t)| \qquad 2.3$$

and the covariance kernal as

$$K(s,t)=E|(X(s)-\mu_s)(X(t)-\mu_t)|=\int_{-\infty}^{-\infty}(x(s)-\mu_s)(x(t)-\mu_t)dF|x(s),x(t)| \quad 2.4$$

where s and t are particular times and μ_s and μ_t the mean values of X(s) and X(t) respectively.

As Kisiel (22) has pointed out, if $\mu_s = \mu_t = 0$ then for $s \neq t$ Eqn. 2.4 yields the autocorrelation function and its graphical expression the correlogram. Also, irrespective of the values of μ_s and μ_t, if $s = t$ then Eqn. 2.4 yields the variance of the process.

If K(s,t) depends only on the difference s-t, i.e., the lag, and if E|X(t)| is also constant for all t, then the process X(t) is said to be covariance stationary and the auto-covariance function is denoted by B(ℓ), where ℓ is the lag. It is assumed henceforth that all stochastic processes will be normalised by subtracting their means so that $\mu_s = \mu_t = 0$. This, of course, does not interfere with their stationarity.

2.2 Variance Spectrum Analysis

Variance spectrum analysis may be considered as the application of generalised harmonic analysis to the study of a stochastic process. Panofsky (31) has stated that the difference between variance spectrum analysis and ordinary Fourier analysis is that the former does not ascribe "the observed variation to a finite number of cycles with discrete periods, but to an infinite number of small oscillations with a continuous distribution of periods." It is assumed

in the following discussion that dominant periodicities, for example annual or diurnal cycles, have been withdrawn from the time series, or do not contribute as much to the total variance of the time series as do the random and non-pure random components.

If $\{X(t) : t \varepsilon T\}$ is a stochastic process which is sampled in the frequency range 0 to ω', then the total variance of the process in this frequency range is given by $H(\omega')$. Obviously $H(\omega')$ is a cumulative distribution function.

If the function $g(\omega)$ is now formed, such that $g(\omega_0) = H'(\omega_0)$, where $H'(\omega_0)$ is the derivative of $H(\omega)$ at ω_0 then $g(\omega)$ is a probability density function and

$$H(\omega_0) = \int_0^{\omega_0} g(\omega)d\omega \qquad 2.5$$

Since it is convenient to work in positive values of frequency, the following even-valued function is defined

$$h(\omega) = \begin{cases} g(\omega)/2 & \text{if } \omega \geq 0 \\ g(-\omega)/2 & \text{if } \omega < 0 \end{cases} \qquad 2.6$$

which is called the spectral density function. Therefore

$$H(\omega_0) = \int_0^{\omega_0} g(\omega)d\omega = 2\int_0^{\omega_0} h(\omega)d\omega \qquad 2.7$$

The relationship between the theoretical auto-correlation function $\rho(\ell)$ and the theoretical spectral density is given by the following Fourier integral transform pair:

$$h(\omega) = \frac{1}{2\pi} \int_{-\infty}^{\infty} \rho(\ell) \exp(-i\ell\omega)\, d\ell$$

$$= \frac{1}{\pi} \int_{0}^{\infty} \rho(\ell) \cos\omega\ell \; d\ell \qquad 2.8$$

$$\rho(\ell) = \int_{0}^{\infty} h(\omega) \cos\omega\ell \; d\omega$$

The plot of $h(\omega)$ versus ω is called the variance or power spectrum, while the plot of $\rho(\ell)$ versus ℓ is called the correlogram. An oscillation of period ℓ^* or frequency $\omega^* = \ell^*/2T_m$ where T_m is the maximum value of the lag, will have a peak on the correlogram at ℓ^* and on the spectrum at ω^*. If the spectrum is constant for all ω, that is the stochastic process is truly random, it is called a white noise spectrum; if the spectrum has a concentration of variance in the low frequencies then the process is called red noise.

2.3 The Estimation of Spectral Density

Before estimates of any of the necessary functions which are needed in time series analysis may be made, it is necessary to call upon the theory of ergodicity and, in fact, make the assumption that the sample time series available is representative of all the possible time series for that time period and spatial area. Hannan (17) has shown that by the ergodic theorem that if $\{X(k)\}$ is covariance stationary and

if {y(k)} is a sample taken on K at k = 1, ... n, then for large n the estimate of the mean of y(k) is given by

$$\bar{y} = (1/n) \sum_{k=1}^{n} y(k) \qquad 2.9$$

and its estimated autocovariance function (acvf), that is the estimated covariance kernal, is

$$C(\ell) = (1/(n-\ell) \sum_{k=1}^{n-\ell} (y(k+\ell)-\bar{y})(y(k)-\bar{y}) \qquad 2.10$$

It is much simpler to calculate $C(\ell)$ by first forming $x(k) = (y(k)-\bar{y})/\sigma$, k = 1, ... n, where σ is the standard deviation of {y(k)} so that $\bar{x} = 0$ and $\sigma^2(x) = 1$ ((19) p.184). This procedure is called standardisation.

If the autocorrelation function (acf) of {X(k)} at lag ℓ is defined as

$$\rho(\ell) = B(\ell)/B(0) \qquad 2.11$$

then the estimated acf is

$$R(\ell) = C(\ell)/C(0) \qquad 2.12$$

where B(0) and C(0) are, respectively, the theoretical and estimated variances of {X(k)}.

Therefore the estimate of the acf, $R(\ell)$, is a function which assumes values not greater than +1, and not less than -1, and is a measure of how points lying ℓ units apart influence each other. It is simply an adaptation of the product-moment correlation coefficient for the analysis of points in time.

A raw estimate of the spectral density at lag ℓ is given by Blackman and Tukey (6) as:

$$V(\ell) = C(0) + 2 \sum_{j=1}^{T_m-1} \{C(j) \cos(\ell j \pi / T_m)\} + C(T_m) \cos(\pi \ell) \qquad 2.13$$

Here $1 < T_m < n$ is the maximum value of the lag and $V(\ell)$ is the raw estimate of the variance spectrum at the frequency $f = \ell/2T_m$. Eqn. 2.13 is simply the discrete form of the expression for $h(\omega)$ in Eqn. 2.8.

However these raw estimates do not give a satisfactory estimate of the true variance spectrum because of the small sample size, and so it is necessary to form a "modified apparent acvf", $C^*(\ell)$, ((6), p.12) and to use this in calculating a smoothed version of the true variance spectrum.

Therefore define

$$C^*(\ell) = C(\ell)\, D(\ell) \qquad 2.14$$

where $D(\ell)$ is a lag window weighing function such that $D(0) = 1$, and $D(\ell) = 0$ for all $\ell > T_m$, where T_m is the maximum lag. Kisiel (22) has suggested that the optimal maximum lag is 10% of the record length.

A commonly used lag window is the "hanning" window:

$$D(\ell) = 1/2(1 + \cos(\pi \ell / T_m)) \quad 0 \leq \ell < T_m \qquad 2.15$$

$$= 0 \quad \ell \geq T_m$$

Therefore the "modified apparent acvf" is

$$C^*(\ell) = 1/2\ C(\ell)(1 + \cos(\ell\pi/T_m)) \quad 0 \leq \ell < T_m \qquad 2.16$$

$$= 0 \qquad \ell \geq T_m$$

The smoothed spectral density estimate is

$$G(\ell) = C(0) + \sum_{j=1}^{T_m-1} C(j)\cos\{(\ell j\pi/T_m)(1+\cos(j\pi/T_m))\} \qquad 2.17$$

Agterberg noted (1):

> "The individual values $G(\ell)$ can be considered as estimators of a smoothed version of the underlying true (variance) spectrum $P_t(\ell)$ with
>
> $$\text{Average } P(\ell) = \int_{-\infty}^{\infty} Q(\ell + \ell_1)\ P_t(\ell)d\ell_1$$
>
> where $Q(\ell)$ is the bell-shaped hanning response function with a main lobe that is $2/T_m$ frequency units wide."

2.4 The Method of Filtering

The derivation of the linear, statistical filter used in this study is due to Agterberg (1) and is based on the theory of Yaglom ((43), Chapter 5).

It is assumed that a signal-plus-noise model represents the structure of hydrological observations. This means that the hydrological variable X(k) is assumed to be composed of two components -- a signal, S(k), and a pure random component that carries either no information or undesired information, N(k) -- the noise. This process is represented by $\{X(k)\} = \{S(k)\} + \{N(k)\}$.

The problem at hand here is given a sample {x(k), k = 1, ...n} to filter out the noise n(k) for all k to leave the signal s(k). The noise may be a sampling error and/or some random fluctuation in sampling that makes the observed values something other than deterministic. The observed values are simply the sum of these two.

In the model it is assumed that {X(k)}, {S(k)}, and {N(k)} are all covariance stationary with zero means. Also it is assumed that the signal and the noise are uncorrelated, i.e., $E|S(k)N(k)| = 0$. Therefore, if $B(\ell)$ represents the theoretical acvf, then

$$\begin{aligned} B_X(\ell) &= B_S(\ell) \qquad\qquad |\ell| > 0 \\ B_X(0) &= B_S(0) + B_N(0) \end{aligned} \tag{2.18}$$

Given a sample {x(k), k = 1, ... n} for which the sample acvf $C_x(\ell)$ and the sample acf $R_x(\ell)$ for $\ell = 0,1,...T$, are known, denoted the sample acvf's for the signal and noise as $C_s(\ell)$ and $C_n(\ell)$ respectively, then $C_s(\ell) = C_x(\ell)$ for $|\ell|>0$.

However to design the filter it is necessary to know $R_s(0)$, the sample zero-lag acf, and $C_s(0)$ which are estimated as follows. Calculate the sample, signal acf by $R_s(\ell) = C_s(\ell)/C_x(0)$, where $C_x(0) = C_s(0) + C_n(0)$ for all $|\ell|>0$, that is assume $C_n(\ell) = 0$ for all $|\ell|>0$. Then $R_s(0)$ equals $C_s(0)$ times a constant. $R_s(0)$ is estimated by finding the least-squares fit to the points $R_s(\ell)$or, in fact, $R_x(\ell)$.

It is now necessary to consider a model for the curve of the correlogram, $R_s(\ell)$. Considering what was said in Section 2.2 on the minor importance of periodic components in this context, there is reason to believe that a simple and adequate model of nonpure random hydrological and climatological time series is the first-order Markov process. Amongst the geophysical time series that have been successfully modelled by a first-order Markov process are daily precipitation (22), the water balance of an esker (12), annual minimum streamflow discharges (24), and evaporation from and the air temperature above a lake (44).

The acf of the first-order Markov process is an exponential function, and the following form used by Agterberg (1) allows an efficient curve-fitting approach

$$R(\ell) = c \exp(-a|\ell|) \qquad 2.19$$

The curve is fitted by least-squares technique to $R_x(\ell)$, $\ell = 1, \ldots m$ where m is that lag such that $R(\ell) > 0$ for all $\ell = 1, \ldots m$ and $R(m+1) \leq 0$. If all values of the acf are positive then $m = T$, the maximum lag.

Therefore $R(0) = c$ is the estimate of $R_s(0)$.

The equations to derive c are developed by taking the natural log of Eqn. 2.19 and performing a simple linear regression, therefore

$$R(\ell) = c \exp(-a|\ell|)$$

becomes

$$\ln|R(\ell)| = \ln c - a|\ell| \qquad 2.20$$

then

$$a = \{\sum_{\ell=1}^{m} (\ln R(\ell)\cdot\ell) - m\cdot\bar{\ell}\cdot\overline{\ln R(\ell)}\}/\{\sum_{\ell=1}^{m} (\ell^2) - m\cdot\bar{\ell}^2\} \qquad 2.21$$

and

$$c = \exp(\overline{\ln R(\ell)} - a\cdot\bar{\ell}) \qquad 2.22$$

To summarise a least-squares line is fitted to the acf $R_x(\ell)$ and extrapolated back to lag 0 where $R_s(0) = c$, $R_n(0) = 1-c$, and $R_x(0) = R_s(0) + R_n(0)$. $R_n(0)$ is a measure of the sampling error and $R_s(0)/R_n(0)$ is called the signal-to-noise ratio.

The filter $b(\ell)$ is that function of ℓ such that for all k

$$s(k) = \int_{-\infty}^{\infty} b(\ell)\ x\ (k+\ell)\ d\ell \qquad 2.23$$

The problem now is to find $s(k)$ in terms of $x(k)$ by the discrete form of Eqn. 2.23

$$s(k) = \sum_{\ell=-\infty}^{\infty} b(\ell)\ x\ (k+\ell) \qquad 2.24$$

so that the sum of the squares of the residuals $n(k)$ is minimised. In the words of Yaglom ((43), p.128) "we may finally reduce the solution of the linear filtering problem to the solution of the following system of linear algebraic equations:"

$$\sum_{\ell=-\infty}^{\infty} b(\ell)R_x(k-\ell) = R_s(k) \qquad 2.25$$

where $k = -h, -h+1, \ldots 0, \ldots .h$.

If a and c of Eqn. 2.10 are known then the solution for Eqn. 2.24 is given by Agterberg (1) as

$$b(\ell) = q \exp(-p|\ell|)$$

where $$p = \sqrt{a^2 + 2ac/(1-c)} \qquad 2.26$$

and $$q = ac/(1-c)p$$

Since Eqn. 2.23 is really a sum of the x(k)'s with the weights $b(\ell)$, then for some lag, $\ell = \alpha$, such that $b(\ell) < \varepsilon$ for $|\ell| > \alpha$, where $\varepsilon > 0$ is arbitrarily small, then

$$s(k) = \sum_{\ell=-\alpha}^{\alpha} b(\ell)x(k+\ell) \qquad 2.27$$

To find α consider $\Sigma H = \sum_{\ell=-\infty}^{\infty} b(\ell)$ and choose $\varepsilon > 0$ and let α be the value such that

$$|\Sigma H - \sum_{\ell=-\alpha}^{\alpha} b(\ell)| < \varepsilon \qquad 2.28$$

This $b(\ell)$ is a symmetrical, bilateral exponential filter such that $b(\ell) \geq 0$ for all ℓ. Then, assuming Eqn. 2.28 holds true, for all $|\ell| > \alpha$ then at least $0 < h(\ell) < \varepsilon/2$. This regulates the error term.

To show that ΣH exists write from Eqn. 2.26

$$\Sigma H = q \sum_{\ell=-\infty}^{\infty} \exp(-p|\ell|)$$

$$= q + 2q \sum_{\ell=1}^{\infty} \exp(-p|\ell|) \qquad 2.29$$

Since $|\exp(-p)| < 1$ then from the sum of a geometric series

$$\Sigma H = q + 2q\{\exp(-p)/(1 - \exp(-p))\} \qquad 2.30$$

A correction is necessary to keep the total sum of the weights constant in going from Eqn. 2.24 to 2.27. To accomplish this introduce $b'(\ell)$ such that

$$b'(\ell) = \Sigma H \cdot b(\ell) / \left(\sum_{\ell=-\alpha}^{\alpha} b(\ell) \right) \qquad 2.31$$

Therefore $\Sigma H = \sum_{\ell=-\alpha}^{\alpha} b'(\ell)$ and the total weight is unchanged. Consequently the final estimate of the signal is

$$s(k) = \sum_{\ell=-\alpha}^{\alpha} b'(\ell) x(k+\ell) \qquad 2.32$$

2.5 The Stochastic Model of the Hydrological Signals

It has been assumed that the model which will best describe the signal is the first order autogressive or Markov process

$$X(\ell) = \rho_1 X(\ell-1) + \eta(\ell) \qquad 2.33$$

whose theoretical acf is given by Bartlett ((5), p.306) as

$$\rho(\ell) = \rho_1^{|\ell|} \qquad |\ell| = 0,1,\ldots T_m \qquad 2.34$$

where ρ_1 is the lag one acf coefficient, and $\eta|\ell|$ is a stationary random function.

The theoretical spectral density is

$$h(\omega) = \frac{(\mathrm{Var}\{X(\ell)\})(1-\rho_1^2)}{\pi(1+\rho_1^2 - 2\rho_1 \cos\omega)} \qquad 0 \qquad 2.35$$

This has a maximum at $\omega = 0$ given by

$$h(0) = \frac{(\mathrm{Var}\{X(\ell)\})(1+\rho_1)}{\pi(1-\rho_1)} \qquad 2.36$$

By converting from angular frequency co-ordinates and by standardising the data so that $\mathrm{Var}\{X(\ell)\} = 1$ the numerical expression for Eqn. 2.35 is

$$h(f) = (1-\rho_1^2)/(1+\rho_1^2 - 2\rho_1 \cos(2\pi f)) \qquad 2.37$$

for $-1 \leqslant \rho_1 \leqslant +1$.

CHAPTER 3

THE EXPERIMENTAL SITE

An experimental site was instrumented at Delta, Manitoba (Figure 3.1, p.35) during the summers of 1970 and 1971 to study diurnal fluctuations of groundwater hydrographs and their climatological causes and effects. The site had been used previously by Gilliland (16) in his studies of the cause of small fluctuations of the water table.

3.1 Geology and Hydrogeology

Delta lies in the middle of the Manitoba plain, whose physiography has been described by Bostock (7) as follows:

> The surface of the Manitoba plain has an elevation of about 800 feet and is very gently undulating to flat. It is largely covered by lakes and includes most of Lake Winnipeg. In the southern part its features have been smoothed over by the deposition of the clays and silts of glacial Lake Agassiz.

The surficial geology of the Delta area (Figure 3.2, p.36) has been described by Gilliland (16):

> The silty clays of Lake Agassiz are overlain by more recent alluvial deposits which grade sharply from sands in the old river channels to silts and clayey silts outside the channels. The alluvial

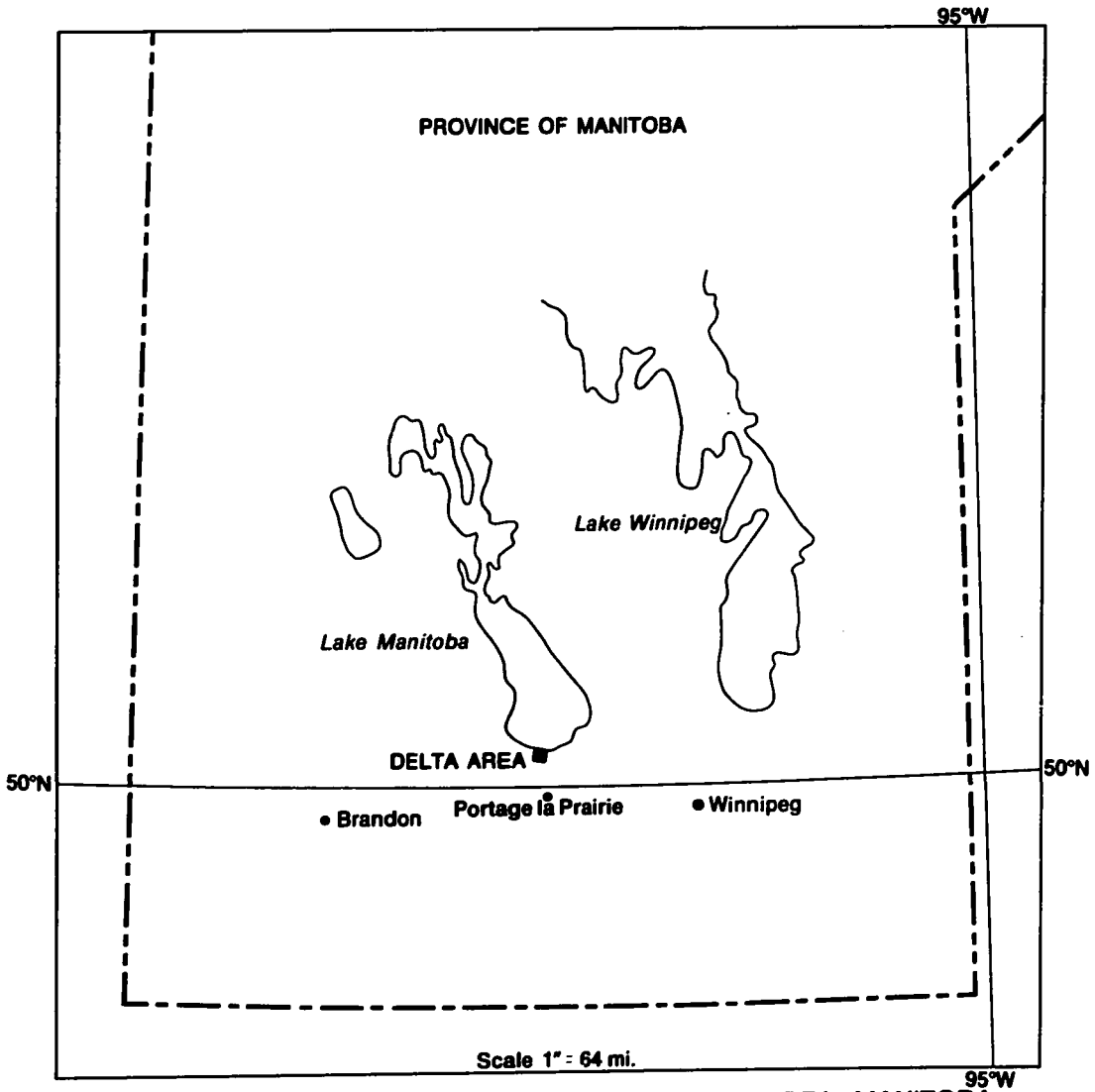

FIGURE 3.1 - MAP SHOWING LOCATION OF DELTA AREA, MANITOBA

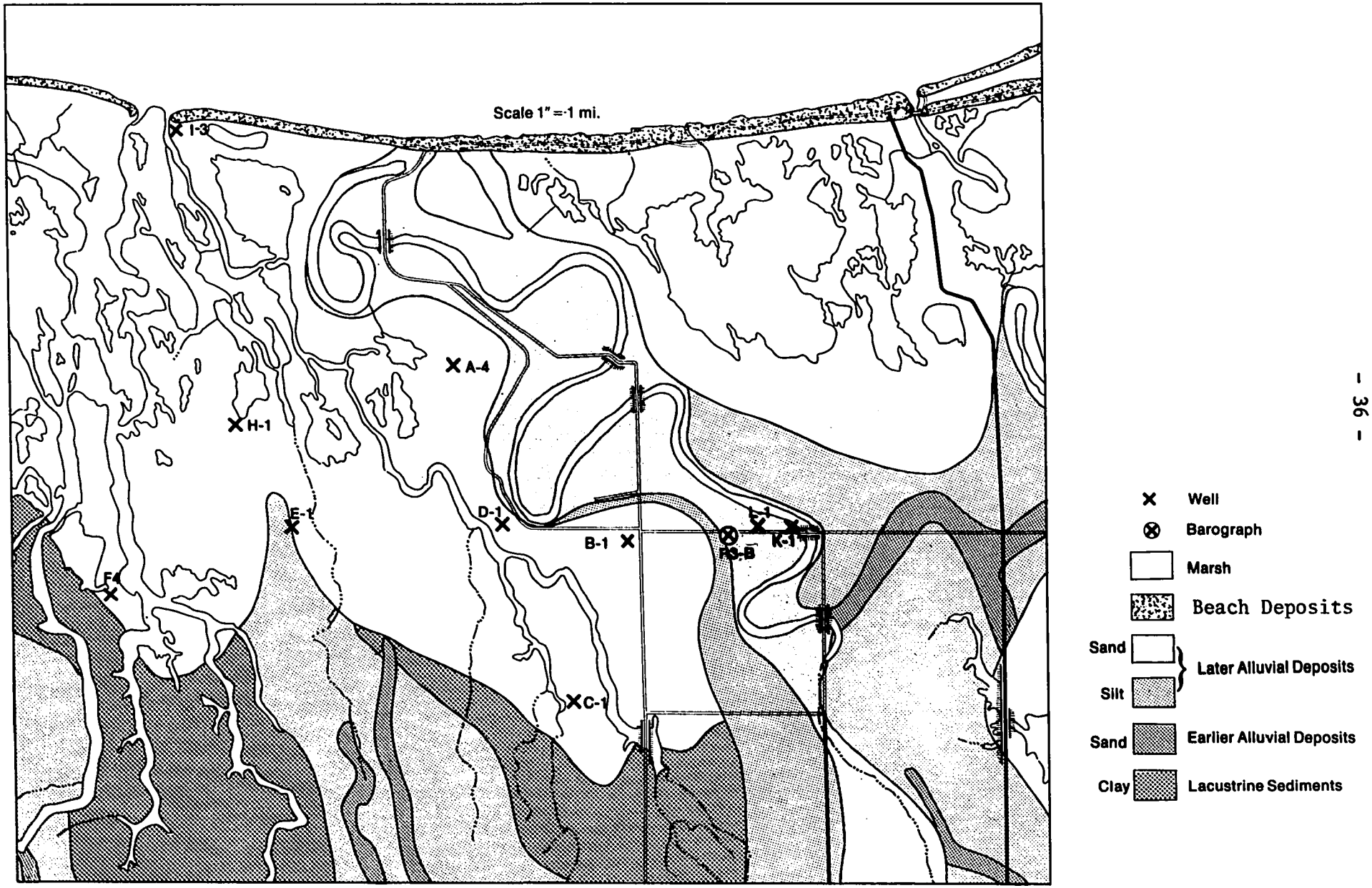

FIGURE 3.2 - GEOLOGY AND WELL LOCATIONS
Delta Area, Manitoba

silty deposits are widespread and, to the eye, uniform.

The Delta area is a groundwater discharge area "in which the water table lies beneath both the mean level of Lake Manitoba and the piezometric surface of the underlying bedrock aquifer" (16). The area is drained by several channels which lead to Lake Manitoba and which are ephemeral, flowing only after snowmelt in the spring.

Each summer since 1967 various existing observation wells have been instrumented with Leupold Stevens type F water level recorders. Lithological logs and details of the well construction are given in Appendix A, however, a brief description of each is presented.

Well K-1 sits in an ephemeral stream channel composed of alluvial sands resting on clays and silts (Figure 3.2, p.36). Well D-1 stands on relatively high ground between two ephemeral stream channels and penetrates seven feet of alluvial silts and clays which sit on top of the Lake Agassiz clays. Although D-1 is in the groundwater discharge area of the regional flow system, it probably forms an ephemeral recharge area for a local flow system during wet spells (Figure 1.1, p.3).

In his time series analysis of water-level fluctuations at Delta, Gilliland (16) assumed that each ground-water hydrograph, H(t), was composed of a sinusoidal, periodic signal, S(t), and a Gaussian random noise, N(t). By cross-

correlating the hydrographs with a diurnal, unit impulse, i.e., one with a period of one day, and then computing theoretical and actual, signal-to-noise ratios, Gilliland was able to identify which wells were fluctuating due to diurnal, evapotranspirative effects. Although the evapotranspirative signal was indeed sinusoidal, Gilliland found that the noise was not Gaussian and attributed it in part to natural recharge by rainstorms. Those wells with sinusoidal amplitudes of the same order as the product of their barometric efficiency and the amplitude of the fluctuation of the barometric pressure were assumed to be responsive to barometric rather than evapotranspirative effects. Both K-1 and D-1 were identified as fluctuating due to evapotranspiration.

Furthermore Gilliland showed that for wells with water levels fluctuating due to evapotranspiration, the phase and the amplitude of the fluctuations were linear functions of the depth, indicating that the transport of water to the surface from the water table is a quasi-linear process when long (approximately 100 days) time periods are considered.

3.2 Climatology

The climate of Southern Manitoba is typically continental -- warm and humid in the summer, cold and dry in the winter. The summer climate is summarised in Figure 3.3. p.39.

There are various ways of demonstrating this continentality. Barry and Chorley ((4), p.197) showed that by

FIGURE 3.3

Summer Climate of Southern Manitoba, 1967

	June	July	Aug.	Sept.
Rainfall in inches*	1.08	3.24	1.39	0.40
Mean Daily Temp.* (deg. F)	62.6	67.9	64.7	60.3
Class A Pan Evaporation (in)**	7.11	8.06	7.47	6.39

*Indicates measured at Portage la Prairie

**Indicates measured at Gimli

Source: Monthly Records, Meteorological Observations in Canada, Canada Department of Transport, Meteorological Branch, Toronto.

use of Conrad's index, which depends on the annual temperature range and the latitude, that Manitoba has the strongest continentality of anywhere in North America south of the 60th parallel. Polowchak and Panofsky's (34) spectral analysis of daily temperatures showed that the geographical distribution of summer and winter variance in North America is also a continentality index, in that the variance maxima are concentrated from Ontario to Alberta. In this case the spectra are expressing the pronounced fluctuations in daily climate that is the essence of a continental climate.

The precipitation and moisture balance regime of the Prairie Provinces is dictated by the summer precipitation, which accounts for 40% of the annual total. According to Barry and Chorley ((4), p.201) the wettest period is "commonly in late summer or autumn when depression tracks are in higher middle latitudes."

At K-1 a climatological station was established to continuously record barometric pressure, relative humidity, air temperature, and precipitation. The instruments employed were, respectively, a Short and Mason microbarograph, a Lambrecht hygrothermograph and a Kahlsico Hellman raingauge. Furthermore a Class "A" U.S. Weather Bureau Evaporation Pan was installed to measure hourly, free-surface evaporation using an electronic sensor.

3.3 Vegetation

Grasses of the genuses Carex and Scripus are predominant at the Delta site.

CHAPTER 4

DATA PROCESSING AND ANALYSIS

4.1 Data Processing

Observation-well hydrographs for the summers of 1967-1971 at Delta were examined for continuity and quality. This involved selecting only those periods of record, showing diurnal fluctuations, which lacked gaps due to instrument malfunction and for which the pen-trace quality permitted accurate estimates of R and Δs. On this basis the following "evapotranspiration seasons" were chosen for analysis -- June 1 to September 21, 1968 at K-1, June 16 - September 10, 1970 at D-1, and June 15 - September 3, 1971 at D-I.

Values of R and Δs of Eqn. 1.1 were taken from the hydrographs and used as input to computer program WHITE (Appendix B), which computed daily values of Q, the groundwater evapotranspiration. On those days on which the hydrograph rose due to rainfall infiltration or to a Lisse Effect and thereby obscured the true value of R, the groundwater inflow rate, R was set equal to zero. This involved 17% of the values at K-1 in 1968 and 12% of the values for 1970 and 1971 at D-1.

Values for the specific yield of the aquifers, S_y, at K-1 and D-1 were taken from data suggested by Meyboom (30). K-1, being a fine-grained alluvial sand, was given a specific yield of 15%, while D-1, being an alluvial clayey silt, was given a value of 10%.

The climatology station at K-1 provided the data for the calculation of mean daily temperature ($\overline{T}$) and daily precipitation ($\overline{P}$) for the summers of 1970 and 1971. For the summer of 1968 values of $\overline{T}$ and $\overline{P}$ for the Delta Wildfowl Research Station, two miles north of K-1, were taken from the Meteorological Service's Monthly Record (3).

4.2 Identification of Nonrandom Components

Time series of Q, R, $\overline{T}$ and $\overline{P}$ for the three seasons (Appendix C) were first standardised by subtracting their means and dividing by their standard deviations. Henceforth these shall be referred to as Q(t), R(t), $\overline{T}(t)$ and $\overline{P}(t)$ respectively. This necessarily made the variance of each variable, C(0), equal to unity, with mean zero. The sample acfs of these series were computed by Eqn. 2.10, which is strictly the acvf however since C(0) = 1 by standarisation, then $R(\ell) = C(\ell)$ (see Eqn. 2.12). Estimates of the spectral density were computed by Eqn. 2.17. The theoretical acf, $\rho(\ell)$, was computed by Eqn. 2.34, while the theoretical spectral density, h(f), was computed by Eqn. 2.37. These computations were performed by program SPECTRA (Appendix D).

A test of significance for $R(\ell)$ has been given by Eagleson and Lariviere (11) as

$$r_k^* = t_p/(v - t_p^2)^{1/2} \qquad 4.1$$

where v is the number of degrees of freedom = $n-\ell-2$, t_p is

the Student's variable at exceedence probability, 1-P, r_k is the value of the acf at lag k which must be exceeded for significance at the chosen level P. For a nonrandom time series v is replaced by v' such that

$$v' = (n-\ell-2)/(1+2r_1^2+2r_2^2+ \ldots..) \qquad 4.2$$

However if the time series is assumed to be generated by a first-order Markov process then

$$v' = (n-\ell-2)(1-r_1^2)/(1+r_1^2) \qquad 4.3$$

The results of that part of the thesis directly concerned with the identification of nonrandom components in the time series are shown in Figures 4.1 to 4.8, pages 44 - 49. Each figure shows either the sample correlograms or spectra of a particular variable over the three seasons. The correlograms, Figures 4.1 to 4.4, pages 44 and 46, show $R(\ell)$ and $\rho(\ell)$, with the aforementioned significance test calculated for various lags by Eqn. 4.1. The equation of the stochastic model (Eqn. 2.33) is also listed, with its acf, $\rho(\ell)$, shown by the dashed line.

The spectra, Figures 4.5 to 4.8, pages 46 - 49, show values of $G(\ell)$ and $h(f)$. The x-axis of the spectrum is calibrated in both frequency units (cycles per day) and in periodic units (days per cycle).

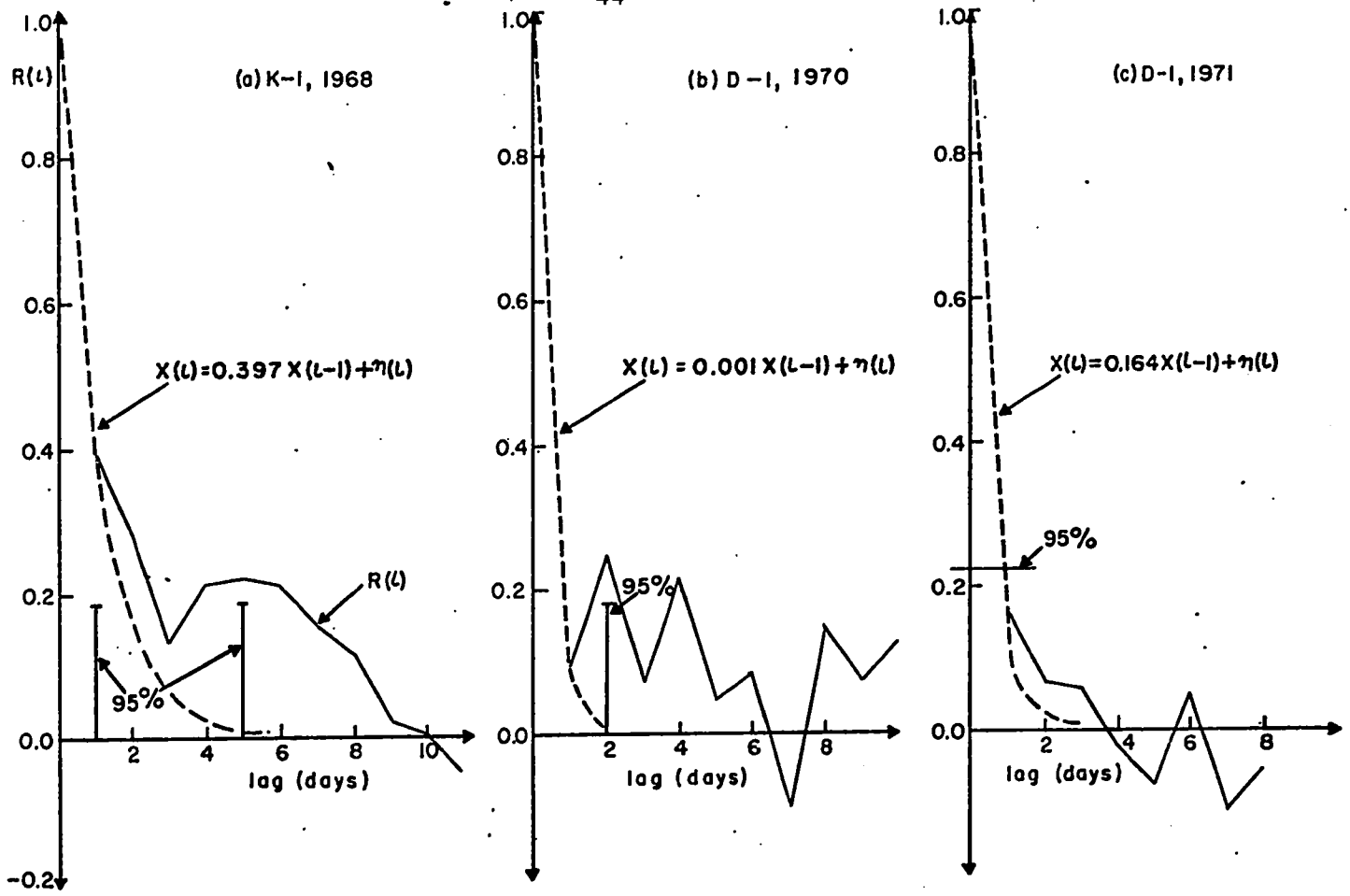

FIG. 4.1 CORRELOGRAMS OF Q

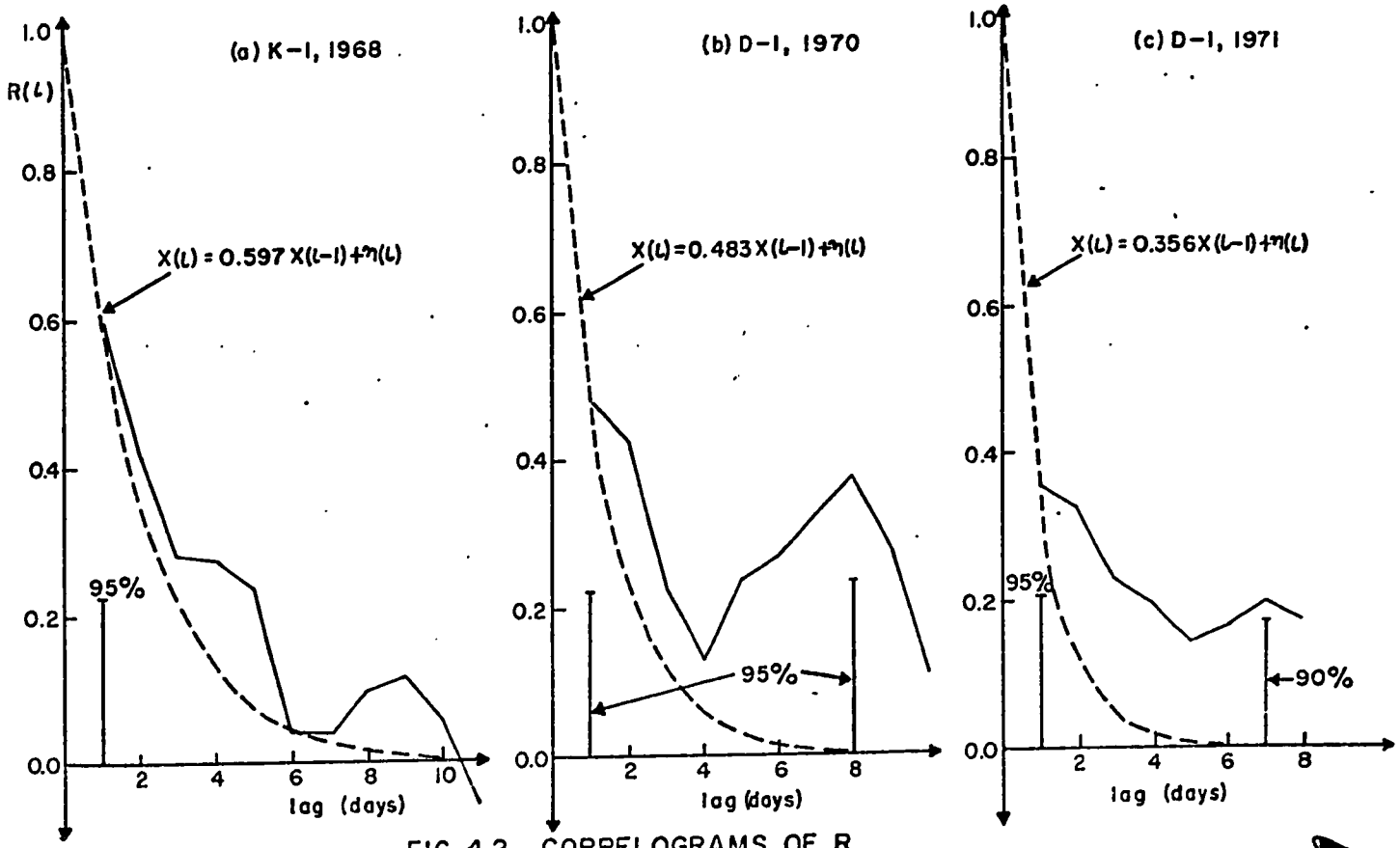

FIG. 4.2 CORRELOGRAMS OF R

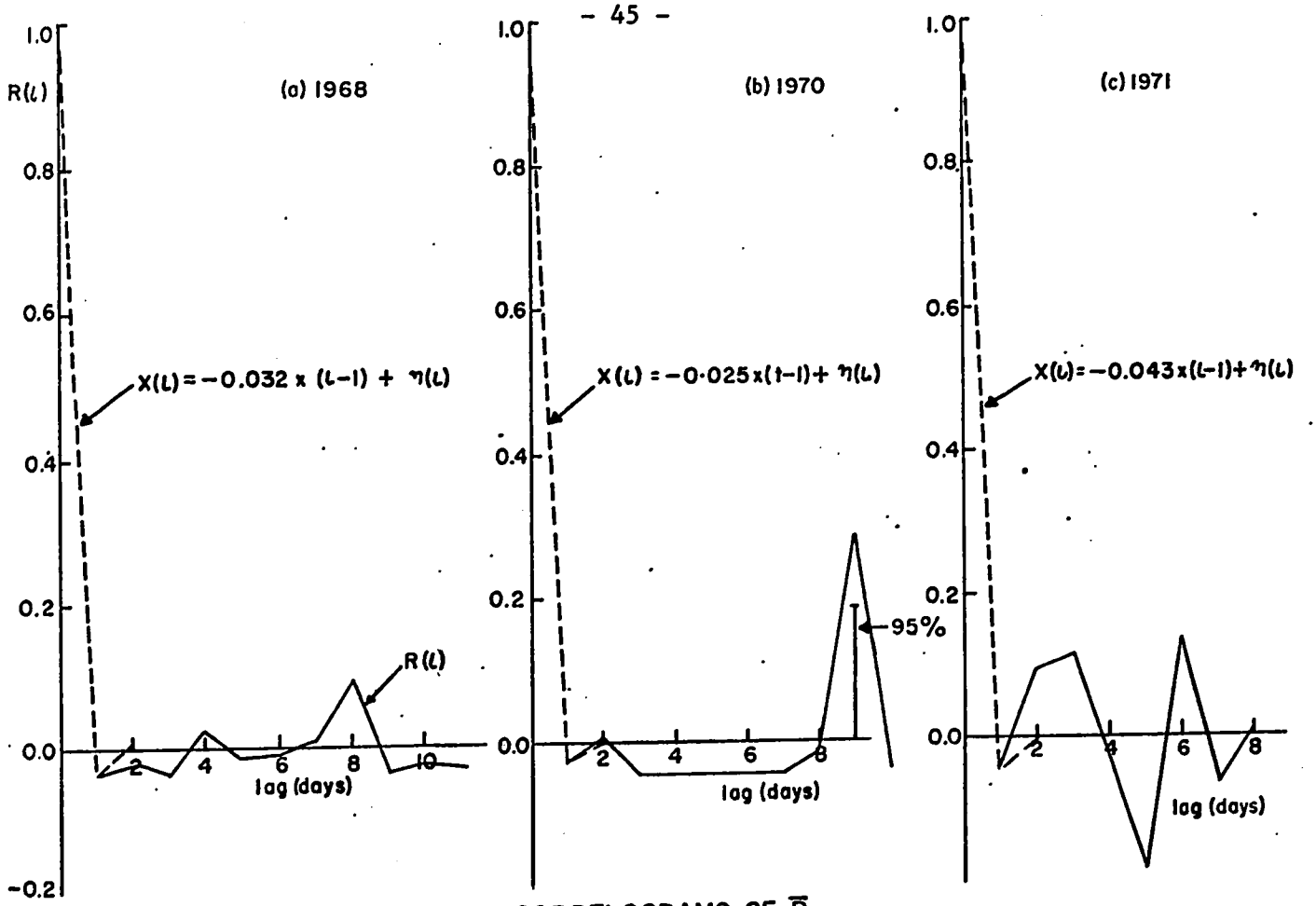

FIG. 4.3 CORRELOGRAMS OF $\overline{P}$.

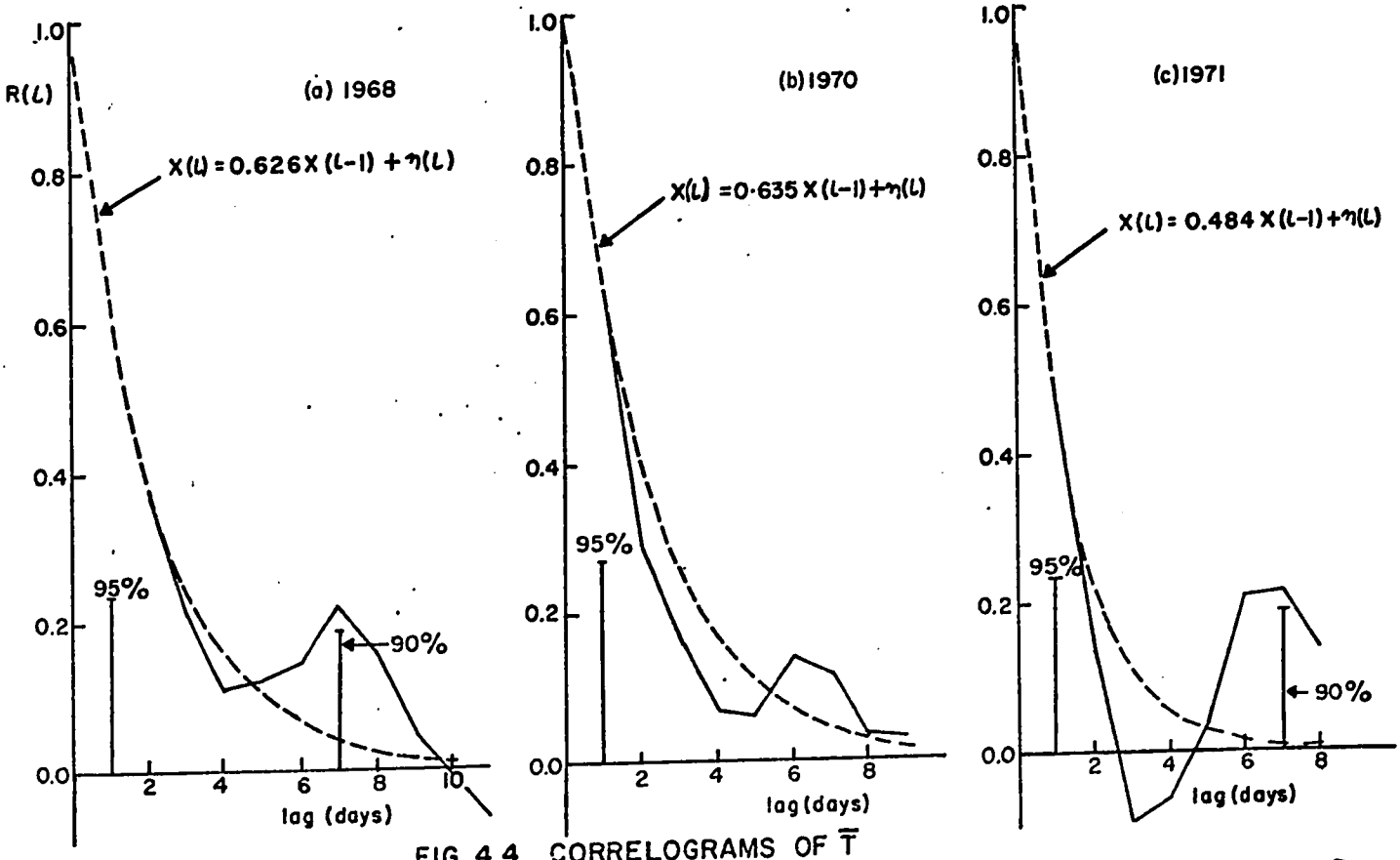

FIG. 4.4 CORRELOGRAMS OF $\overline{T}$

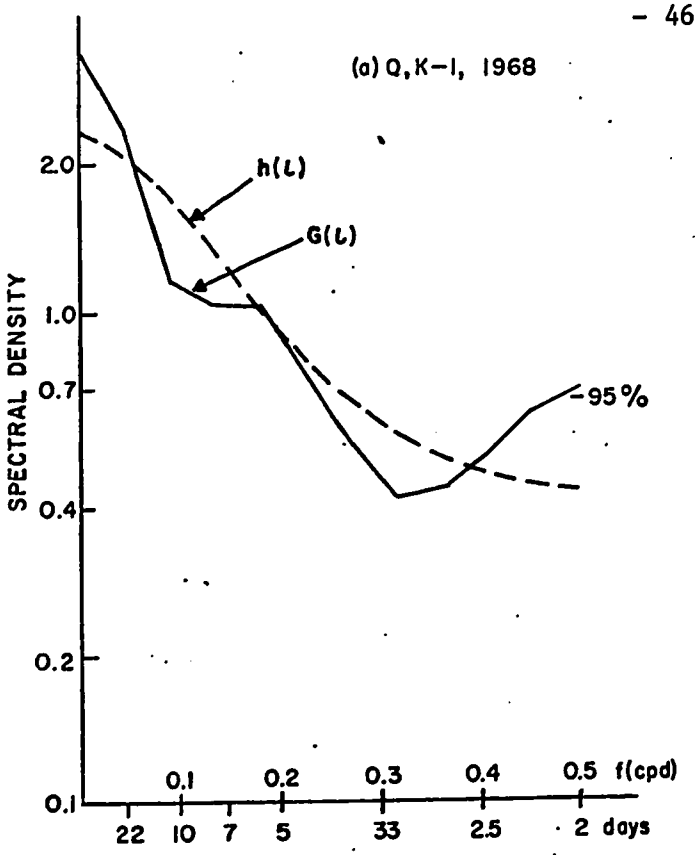

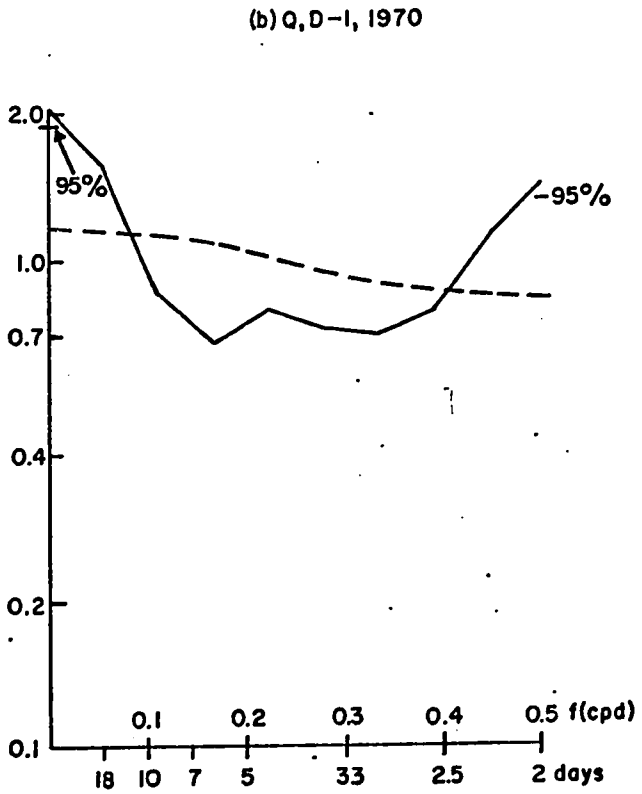

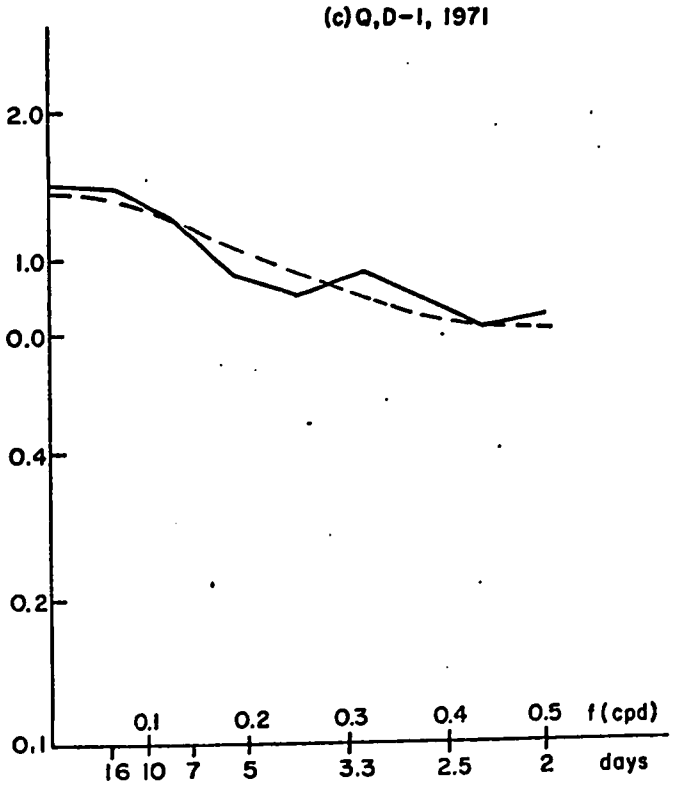

FIG. 4.5 SPECTRA OF Q

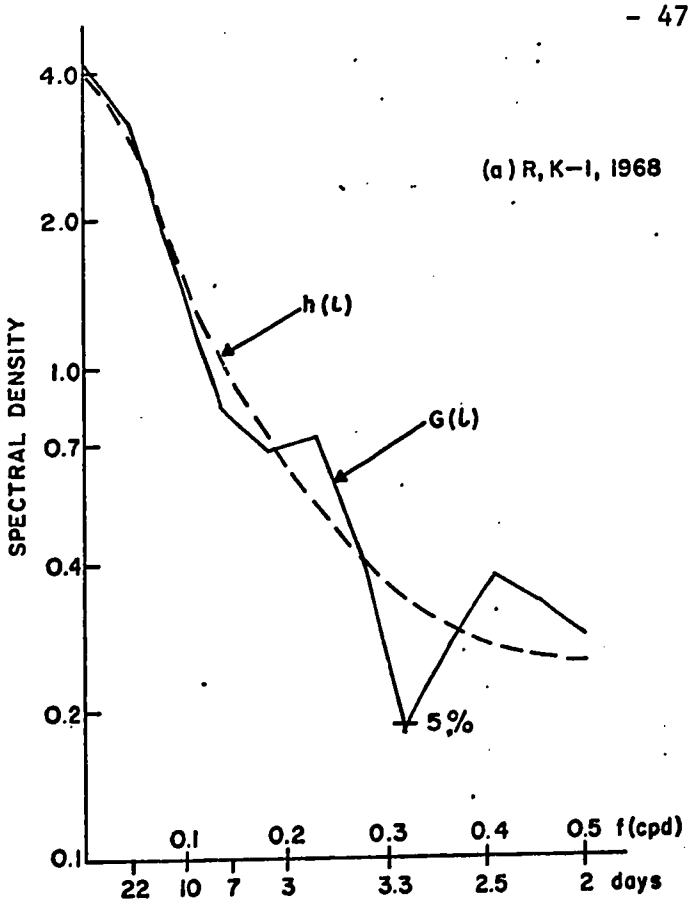

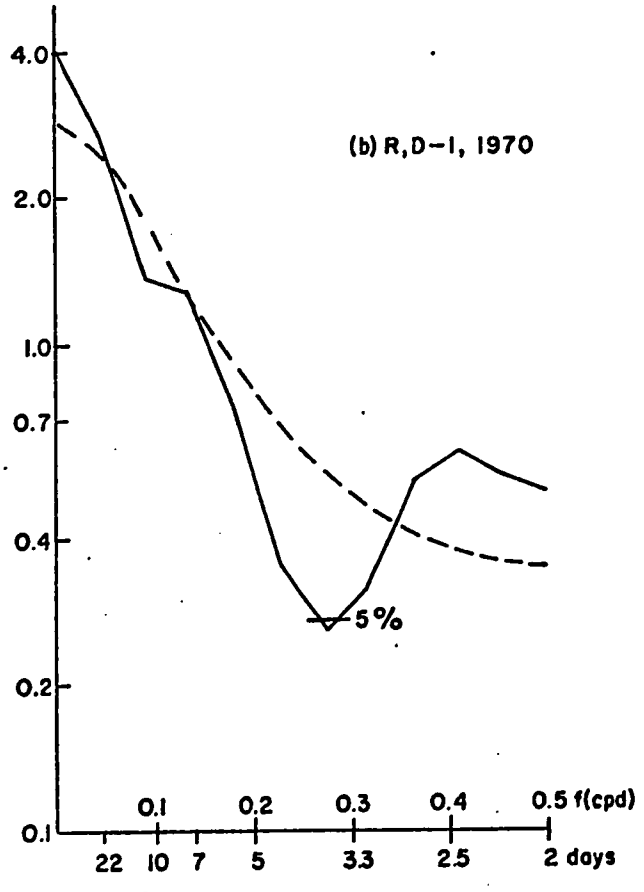

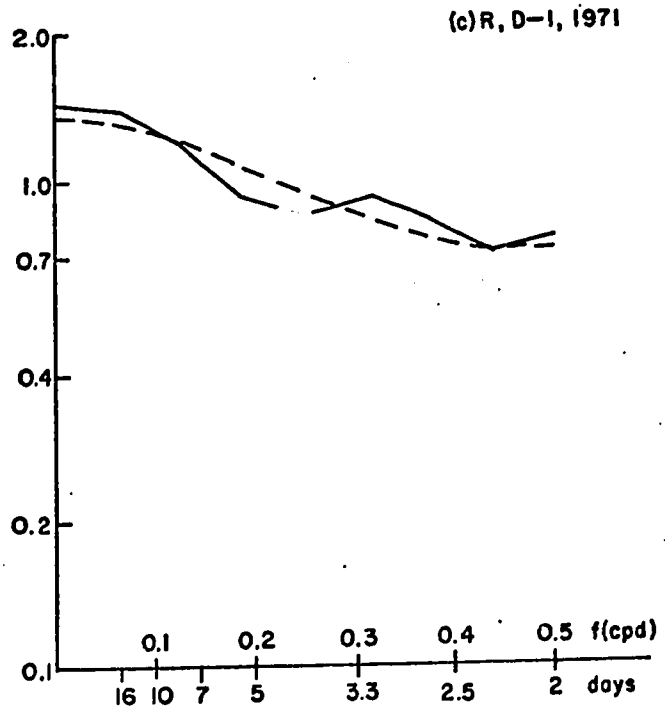

FIG. 4.6 SPECTRA OF R

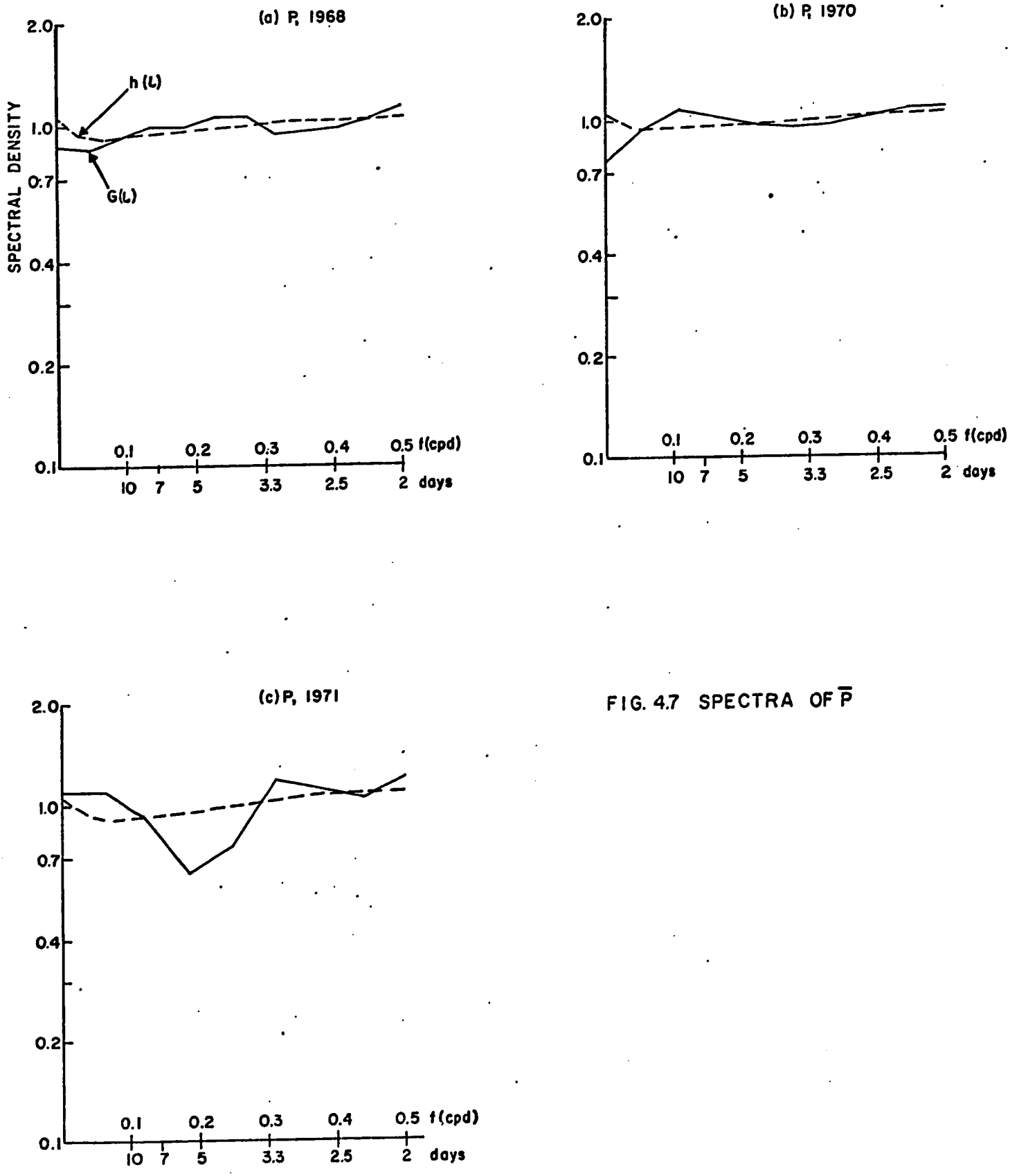

FIG. 4.7 SPECTRA OF $\overline{P}$

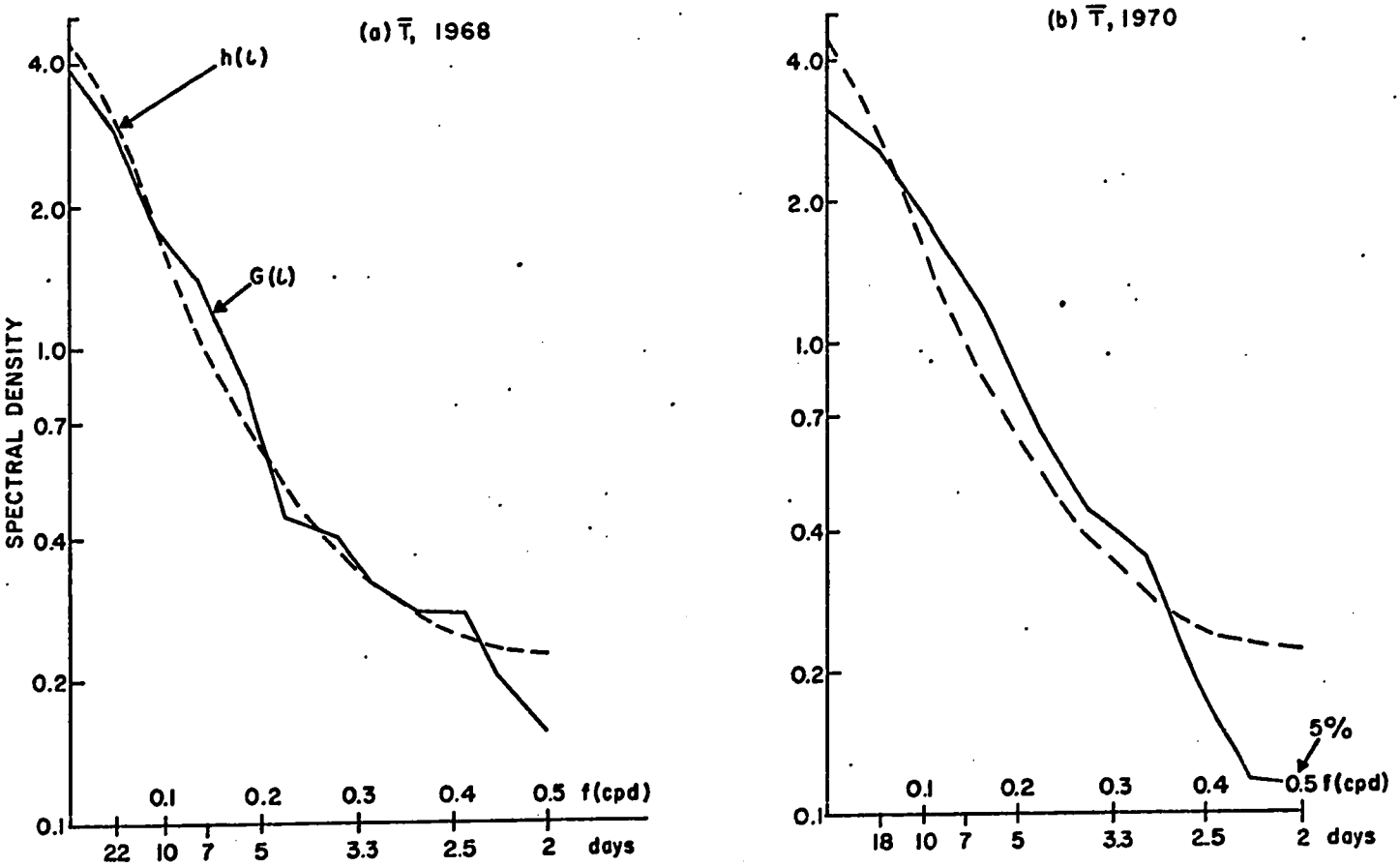

FIG. 4.8 SPECTRA OF $\overline{T}$

4.3 Stochastic Modelling of Q(t) and R(t)

In order to test the adequacy of the proposed stochastic models of the signals of Q(t) and R(t) (Eqn. 2.33), it is necessary to apply statistical tests to both the correlograms and the spectra.

The small sample size (n) of most geophysical records leads to less damping in the sample correlogram than in the theoretical one, because the sample autocorrelation coefficients are inflated by sampling errors which would approach zero as n approaches infinity (24). This disadvantage is part of the reason why the statistical testing of correlograms is less satisfactory than that of spectra.

Quenouille (36) has suggested the following goodness-of-fit test for Eqn. 2.33, the stochastic model of the signals, such that the value of chi-square associated with the kth order autocorrelation coefficient is given by

$$\chi_k^2 = (n-k)R_k^2/(1-R(1)^2)^2 \qquad 4.4$$

where $R_k^2 = R(k) - 2R(1)R(k-1) - R(1)^2R(k-2)$

If

$$\sum_{k=1}^{T_m} \chi_k^2 > \chi_{T_m}^2(\alpha) \qquad 4.5$$

where the right-hand term is the value of the chi-square with confidence level α and T_m degrees of freedom (T_m = the maximum lag of the acf), then the first-order Markov process is

rejected. Figure 4.9 (p.52) shows the results of this goodness-of-fit test.

A further test of the suitability of the proposed stochastic model may be carried out by using Tukey's sampling theory (22). This test involves determining whether any of the sample spectrum estimates are significantly different from the proposed theoretical spectrum value of the first-order Markov process (Eqn. 2.37). Confidence limits for chi-square-distributed values of $G(\ell)$ have been given by Panofsky and Brier ((32), p.145). By using the computed 95% confidence level it is possible to identify significant spectral peaks, and by using the 5% confidence level it is possible to pick out significant spectral gaps. There is only a 5% probability that a sample spectrum estimate will be larger than the 95% confidence level and smaller than the 5% level. The six significant spectral estimates are shown in Figures 4.5 to 4.8, pages 46 - 49, by horizontal dashes with the accompanying confidence level.

4.4 Development of the Statistical Filter

Program SPECTRA was so written that after analysing the time series of Q and R for nonrandom components it would then subject each to the method of statistical filtering described in Section 2.4. Values of a and c, the regression coefficients in Eqn. 2.19, were computed by Eqns. 2.20, 2.21 and 2.22. In this way the acf of the signal was built into

Time Series	$\sum_{k=1}^{T_m} \chi_k^2$	$\chi^2_{T_m}$ (0.1)	Results at 90% level
Q,K-1, 1968	25.17	17.28	rejected
Q,D-1, 1970	12.72	14.68	accepted
Q,D-1, 1971	4.47	13.36	accepted
R,K-1, 1968	50.02	17.28	rejected
R,D-1, 1970	33.89	14.68	rejected
R,D-1, 1971	15.79	13.36	rejected

Figure 4.9 Goodness-of-Fit Test for proposed Stochastic Model

the filter, which was then derived by Eqn. 2.26. The error term, ε (Eqn. 2.28), was fixed at 0.05. Figure 4.10 lists values of a, c, p, and q for each time series of Q and R.

By filtering the standarised values of Q(t), and R(t), the signal, s(k) of each series is given. Figures 4.11 to 4.13, pages 55 - 57, show the seasonal pattern of the filtered values of Q and R, with $\overline{T}$, $\overline{P}$ and weekly water table depths. Periods of infiltration and Lisse effects are noted by 'I' and 'L' respectively.

Time Series	Sample Size (n)	Mean	Variance	a	c	p	q
Q,K-1, 1968	113	.012	.00007	.224	.487	.692	.309
Q,D-1, 1970	87	.010	.00005	.120	.163	.248	.095
Q,D-1, 1971	81	.004	.00001	.511	.239	.763	.211
R,K-1, 1968	113	.000	.00001	.259	.608	.933	.431
R,D-1, 1970	87	.000	.00001	.673	.374	.291	.138
R,D-1, 1971	81	.000	.00000	.129	.366	.408	.183

Figure 4.10 Statistics of Q(t) and R(t)

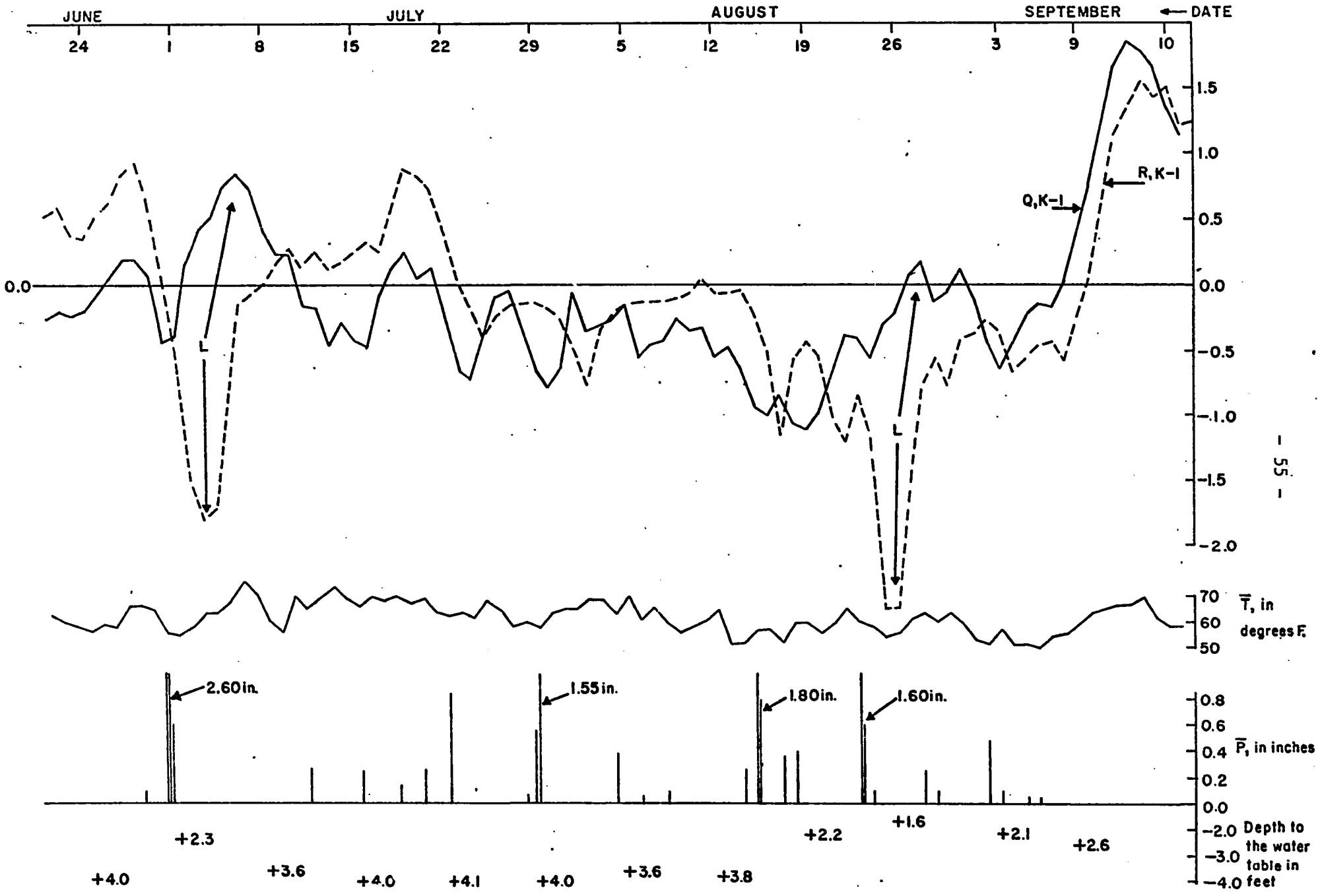

FIG. 4.11 EVAPOTRANSPIRATION SEASON, 1968

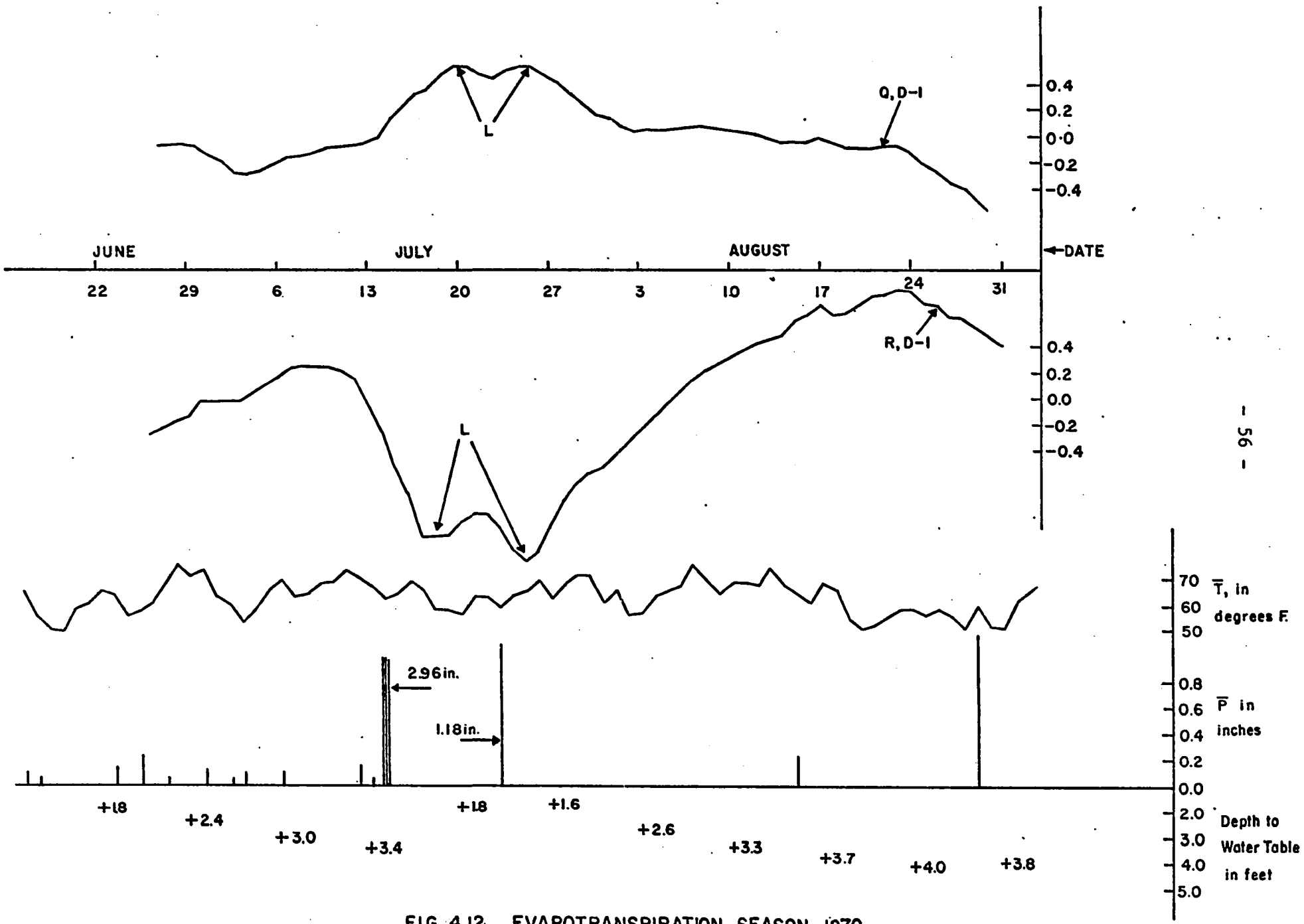

FIG. 4.12 EVAPOTRANSPIRATION SEASON, 1970

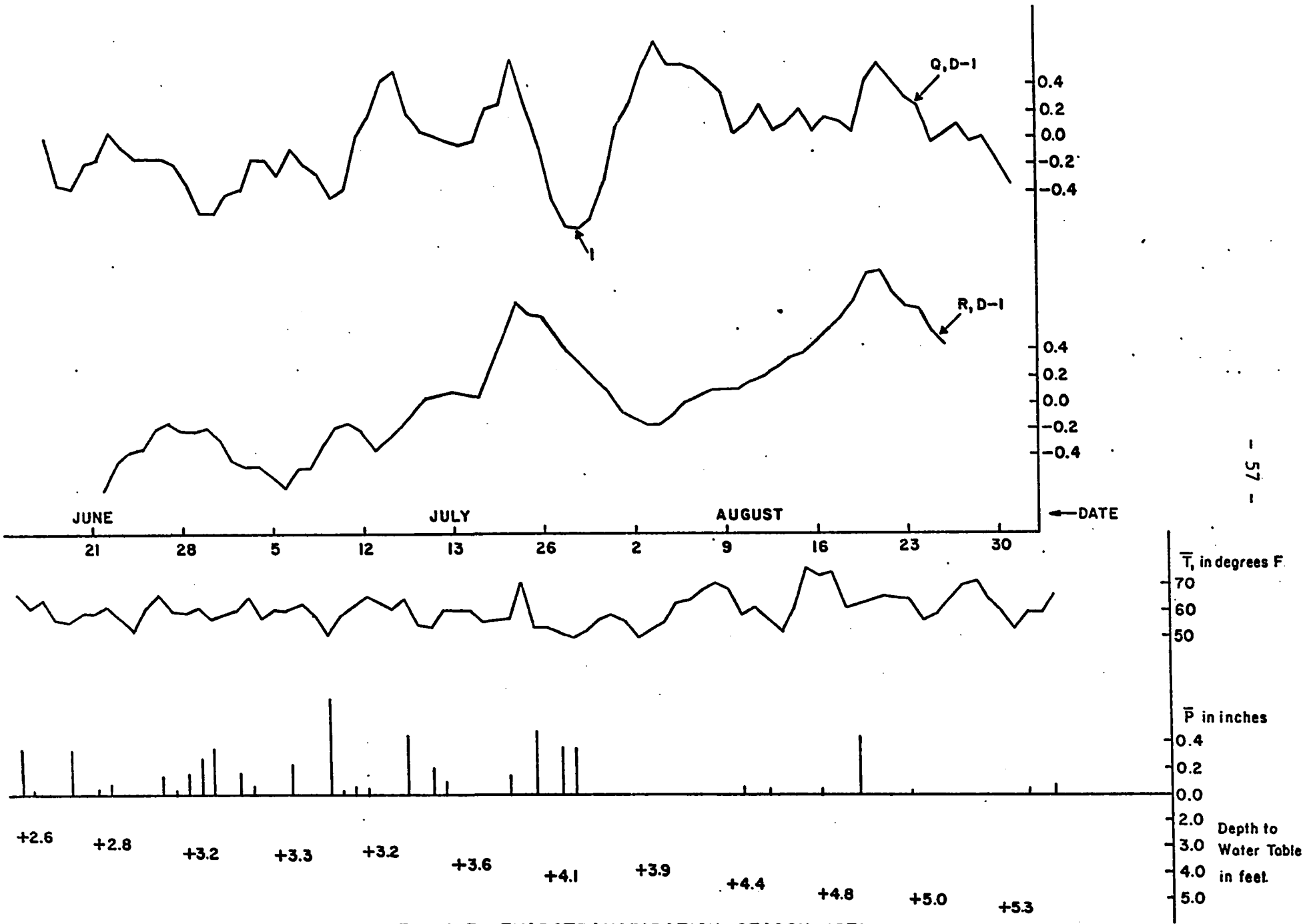

FIG. 4.13 EVAPOTRANSPIRATION SEASON, 1971

CHAPTER 5

DISCUSSION

The procedure described in the last chapter assumed that the trend and periodic components of the time series of Q and R were absent. That is it assumed Q(t) and R(t) to be random, which was then checked by the computation of correlograms and spectra and found to be incorrect. The tools by which the nonrandomness was identified were then used to filter out this nonrandom signal, and were further used to determine whether the proposed stochastic model was suitable.

5.1 Assumptions

Two assumptions were made by White (42) in deriving Equation 1.1. In the first case he assumed that R, the groundwater inflow rate, remained constant throughout the day and, second, he implied that there must be instantaneous discharge of Q, the evapotranspiration from the groundwater body. Hydrograph analysis of K-1, 1971, showed that while there is persistence between values of R one day apart it was quite common for the rising limb of the hydrograph in the early morning to have a different R than that of the rising limb late that night (Figure 1.2, p. 7).

Similarly the second assumption is not strictly fulfilled since the vertical transport of water from the water table to the plant stomata takes place in a finite time (29).

Nevertheless the nonfulfillment of these two assumptions is not of critical importance since the quantities of Q and R are not the primary interest in the study. All that is required is a consistent method to permit analysis of their time distribution.

There are several assumptions concerning Agterberg's filter which merit discussion. One of these is conceptual, that of the validity of the signal-plus-noise model, while the other are concerned with the stationarity, normality, and ergodicity of the data.

The validity of the signal-plus-noise model, which has already been touched upon in Section 2.4, may be confirmed in the light of the errors just discussed which are introduced in extracting the data from the hydrographs. These errors may then be considered as white noise which is uncorrelated with the signal and must be filtered out. Furthermore there are the actual sampling errors incurred at the observation well.

Covariance stationarity may usually be approximated by standardising the time series, furthermore the dynamic equilibrium model of the hydrologic regimen of the discharge area presented in Section 5.6 suggests that the data is at least homogeneous. This model states that the water table will fluctuate in a zone of limited depth beneath the ground surface, consequently extreme nonstationarity in the Q and R time series, both of which depend on depth, will be avoided.

The normality of the data is generally regarded as important in the significance and the goodness-of-fit tests. While Q, 1968 and Q, 1971 of the hydrogeological variables were both skewed, McDonald (26) has presented convincing evidence that the climatologist and hydrologist interested in correlation analysis need not be overly concerned when their data does not approximate a bell-shaped curve.

Ergodicity, as Kisiel (22) has noted, is impossible to establish since the ensemble of samples of any hydrologic process is never available. Consequently an attempt to satisfy ergodicity was made by using three evapotranspiration seasons from two sites in the discharge area. Such an approach should minimise the liklihood of purely local effects having a dominant effect on the results.

5.2 Nonrandom Climatological Components

The two climatological variables responded quite differently to the weather and atmospheric circulation associated with each of the three summer periods. As Landsberg and his co-workers (23) noted the three precipitation seasons each have their own spectral signature which are all basically random (Figure 4.7, p.48). The correlograms (Figure 4.3, p.45) have only one statistically significant value, R(9) in 1970, and this is a chance correlation due to the occurrence of two of the summer's major storms being nine days apart.

In contrast to this strong randomness, the temperature correlograms (Figure 4.4, p.45) showed one- and two-day persistence, which can be viewed as a measure of the local residence time of air masses, and significant 6 to 7 day cycles, due to the aforementioned waves in the westerlies. The temperature spectra (Figure 4.8, p.49) are all rather similar, especially 1968 and 1970, with most variance concentrated in the low-frequency or long-period range of greater than ten days, the so-called red noise spectrum.

The summer of 1968 was a particularly interesting one with strong westerly flow from June to mid-August which weakened with the growth of high-latitude blocking leading first to a trough (Sept. 3-7) and then to a dominant ridge over central North America in mid-September (2,35). The westerly flow and the high-latitude blocking account for the significance of R(7) in Figure 4.4a, p.45, while the anticyclone of September gave the fine hot weather which produced the large values of Q (Figure 4.11, p.55). The dominance of the low frequencies in the spectrum is probably due to a trend, which in reality is the summer portion of the annual temperature cycle, however since the cycle is not complete it is ascribed to a zero frequency oscillation.

The persistent, continental, anticyclonic conditions of late July and August, 1970 (40) resulted in two-day persistence at Delta (Figure 4.4b, p.45) and a concentration of variance in the low-frequency portion of the spectra (Figure 4.8b, p.49), as predicted by Dickson (3).

Given what has been said above and due to the absence of published analyses of this summer's climate at the time of writing (September 1971), it is possible and desirable to speculate briefly on the nature of the climate of summer 1971 by analysing the appropriate correlogram (Figure 4.4c, p.45) and spectrum (Figure 4.8c, p.49). Unlike 1970 the correlogram exhibits one-day and not two-day persistence and a stronger 6 to 7 day peak. The spectrum has a damped low-frequency component. These factors suggest generally cool and very changeable weather dominated by the westerlies associated with the noticeable absence of a strong continental, summer anticyclone.

5.3 Nonrandom Hydrogeological Components

It is now opportune to recall the concept of dynamic equilibrium associated with Freeze in Section 1.1. The groundwater flow system is in dynamic equilibrium and responds to changes in input and output, and therefore storage, by adjusting the piezometric head distribution throughout the flow system. This response is manifested by daily fluctuations in the values of Q and R.

Considering Q first, the correlograms (Figure 4.1, p.44) show differing responses to temperature. Only in 1968, a year of strong persistence in $\overline{T}$, was there significant persistence in Q. Again only in 1968 was there a significant peak in both Q and $\overline{T}$ in the 5 to 7 day periodicity. The lack of coherence between the peaks, 5 days for Q and 7 for $\overline{T}$,

probably reflects the importance of the depth to the water table. A 7-day cycle of $\overline{T}$ will progressively lower the water table such that, as Gilliland (16) pointed out, the amplitude and phase lag of the groundwater hydrograph undergoing evapotranspiration will be significantly altered.

It should be pointed out here that most of the significant acf estimates for 1970 are intimately connected with the two Lisse effects which dominated Q and R that summer. The two- and four-day peaks in Figure 4.1b, p.44, are due to the chance occurrence of two major storms eight days apart. Generally, with one exception, the correlograms for Q and R, 1970 do little to help develop a more general understanding of the role of climate in a groundwater discharge area.

The exception noted above refers to the persistence of the first three autocorrelation coefficients of R. This is permitted by the large storage of the flow system and is due to daily extractions of evapotranspiration which is replaced by upward seepage, that is, positive values of R. These positive R's reflect a disturbance in the equilibrium of the flow system, that is previous recharge and/or discharge events, therefore an adjustment on the part of the flow system is required to offset the increase in the head difference between recharge and discharge areas. The adjustment transfers groundwater to the discharge area. An excellent example of this is the period of high R values in September, 1968 following the heavy rains of August (Figure 4.11, p.55).

The large number of zero values of R at D-1 for 1970 and 1971, that is no upward seepage, probably may be explained by the fact that the well is in a slight topographic high and the upward flowing streamlines of the discharge area are diverted to the sloughs on either side of D-1.

The negative values of R are due to the drainage of the water table after Lisse effects or infiltration periods.

5.4 The Stochastic Model of the Signals

To determine the suitability of the proposed stochastic model of the signals, it was necessary to use two kinds of statistical tests.

The results of the chi-square goodness-of-fit test to the correlograms of Q and R gave disappointing results (Figure 4.9, p.52). Only those time series with R(1) less than 0.3 were accepted. Similar results were experienced by Matalas (24) with streamflow discharges. However the key to the results probably lies in the fact that Quenouille (36) designed the test for large sample sizes, by which he meant several hundred values and not just one hundred.

Much more encouraging results were derived when all four variables were subjected to the Tukey sampling theory. As was noted in Section 4.3 only six values in the twelve spectra were significantly different at the 90% confidence level from the spectrum of a first-order Markov process.

In summary the results of the Tukey sampling theory seem to be both more reliable and more positive and it is concluded that, as a visual inspection of the spectra will confirm, the first-order Markov process adequately models $Q(t)$, $R(t)$ and $\overline{T}(t)$, while $\overline{P}(t)$ is obviously random.

5.5 Statistical Filtering of the Signals

The results of the statistical filtering show that two processes act to give seasonal maxima in the Q time series, both occurring in the presence of a shallow water table, that is less than 3 feet, and hot weather.

For 1968 (Figure 4.11, p.55) the maximum Q was produced in September when strong upward seepage at K-1, coupled with daily maximum temperature in the eighties and a water table between 2.6 and 3.2 feet were the principal causes. Late June and mid-July, 1968 showed similar but less important examples of this process.

This process probably accounts for the observations of McDonald and Hughes (25) at Yuma, Arizona (see Section 1.2.4). They noted that the maximum daily amplitude of the diurnal fluctuations of the water table occurred in October, rather than when they expected which was in late July, when the water table was at its deepest. The ideas developed in this thesis suggest that the large groundwater inflow rates of October were a response to the rains of August, September and October which are a regular feature of the climatology of the U.S.

Southwest. These maximum amplitudes were therefore due to the hydrogeological response of the flow system to the climatic stimulae of infiltration in the recharge area and ninety-degree heat of October causing large consumptive use in the discharge area. The amplitudes of July were small compared with those of October because of a lack of recharge due to the early summer drought of Arizona.

The observation well at D-1 showed very different responses during 1970 and 1971 than K-1 in 1968. The evapotranspiration season 1970 (Figure 4.12, p.56) was dominated by two Lisse effects which brought the water table within two feet of the surface, and consequently into the influence of a denser root zone network. Maximum temperature in the seventies and eighties then caused large daily consumptive use. The largest value of Q in 1971 (Figure 4.13, p.57) was on August 4 when infiltration brought the water table to within four feet of the surface. The difference between the response of K-1 and D-1 may reflect the existence of a local flow system at D-1, which was suggested in Chapter 3 of this study.

Therefore large values of Q are a function of hot weather and a factor that brings the water table close to the surface. In one case this factor is due to climatic effects on the recharge area producing large groundwater inflow rates. In the second case it is due to climatic elements affecting the discharge area, the Lisse effect and infiltration.

5.6 The Hydrologic Regimen

In the development of his mathematical model of a groundwater flow system, Freeze (14) had to assume a steady-state water table, which he defended on the grounds that the zone of fluctuation of the water table is small compared with the saturated thickness of the flow system. Results from the present study suggest why this is necessarily true as far as the groundwater discharge area of the flow system is concerned.

In a groundwater discharge area the upper limit of the water table is effectively controlled by groundwater evapotranspiration and lateral base-flow discharge to nearby streams, both of which increase with the shallowness of the water table. The lower limit is controlled by the increase in piezometric head with depth, which suggests that the groundwater inflow rate should also increase with depth to the water table. However, the very factors that control the upper limit of the water table become less important as it is lowered by their action. In one case the rate of groundwater evapotranspiration becomes insignificant compared with groundwater inflow rate at depth, while in the other, lateral baseflow discharge to a stream ceases when the water table falls beneath the base level of the stream. Although these factors become less important with depth, climatic stimulae occur which return the water table to a shallower depth. In one case these stimulae affect the discharge area in the form of the Lisse effect and infiltration, while in the other case

they affect the recharge area whence, by lateral flow, discharge increases in the discharge area.

CHAPTER 6

CONCLUSIONS

Nonrandom components associated with the weather and circulation of the North American summer climate were identified in the time series of mean daily temperature and, in much damped form, in the time series of daily groundwater evapotranspiration. Daily precipitation was random.

The groundwater variables were adequately modelled by a first-order Markov process.

Statistical filtering of the hydrogeological variables showed that seasonal maxima in the daily groundwater evapotranspiration time series occurred in the presence of hot weather and a shallow water table. Shallow water tables in the groundwater discharge area were associated with either strong, upward groundwater flow due to a recharging of the flow system, or infiltration or the Lisse effect raising the water table.

Results from the study explain why the water table fluctuates within a small range of depth in the groundwater discharge area, a major assumption of the steady-state, mathematical model of groundwater flow systems.

The methods used in this study should find ready application in suggesting sampling times for observation-well networks, and for studying nonrandom components affecting the water balance of regions.

REFERENCES

1. Agterberg, F. P., Stochastic model for the deposition of varves in glacial Lake Barlow-Ojibway, Ontario, Canada. Can. Journal of Earth Sciences. Vol. 6, No. 4, 1969, pp.625-652.

2. Andrews, J. F., The Weather and Circulation of August 1968. Monthly Weather Review, Vol. 96, No. 11, 1968, pp.826-832.

3. Anon, Monthly Record, Meteorological Observations in Canada, Canada Dept. of Transport, Met. Branch, Toronto.

4. Barry, R. G. and Chorley, R. J., Atmosphere, Weather and Climate. Methuen, London, 1968.

5. Bartlett, M. S., An Introduction to Stochastic Processes, Cambridge University Press, 2nd Edition, 1966.

6. Blackman, R. B. and Tukey, J. W., The Measurement of Power Spectra, Dover Books, New York, 1958.

7. Bostock, H. S., Physiographic Subdivisions of Canada, Ch. 2 of R.J.W. Douglas (ed.), Geology and Economic Minerals of Canada, The Queen's Printer, Ottawa, 1970.

8. Canadian Subcommittee on Hydrology, Research Needs in Hydrology in Canada, N.R.C., Ottawa, 1959.

9. Dickson, R. R., On the Relationship of Variance Spectra of Temperature to the Large-Scale Atmospheric Circulation, Journal of Applied Meteorology, Vol. 10, No. 2, 1971, pp.180-193.

10. Dickson, R. R., personal communication, 1971.

11. Eagleson, P. S. and Lariviere, R. F., The Scale of Oceanic Influence on Continental Precipitation, I.A.S.H. Symposium on World Water Balance, Vol. I, Reading, 1970, pp.34-39.

12. Eriksson, E., Groundwater Time Series; An Exercise in Stochastic Hydrology, Nordic Hydrology, Vol. 1, No. 3, 1970, pp.181-205.

13. Eriksson, E., Cross-Spectrum Analysis of Groundwater Levels in an Esker, Nordic Hydrology, Vol. 1, No. 4, 1970, pp.245-259.

14. Freeze, R. A., Theoretical Analysis of Regional Groundwater, Scientifc Series, No. 3, Inland Waters Branch, Ottawa, 1969.

15. Gilliland, J. A., A rigid plate model of the barometric effect, Journal of Hydrology, Vol. 7, 1969, pp.233-245.

16. Gilliland, J. A., Application of Correlation Functions to the Analysis of Groundwater Hydrographs, Unpublished Report, Inland Waters Branch, Ottawa, 1970.

17. Hannan, E. J., Time Series Analysis, Methuen Ltd., London, 1960.

18. Jaworski, J., Evapotranspiration of plants and fluctuation of the groundwater table, I.A.S.H. Symposium, Wageningen, Vol. 2, Water in the Unsaturated Zone, 1968, pp.730-739.

19. Jenkins, G. M. and Watts, D. G., Spectral Analysis and its Applications, Holden-Day, San Francisco, 1968.

20. Julian, P. R., Variance Spectrum Analysis, Water Resources Research, Vol. 3, No. 2, 1967, pp.831-845.

21. Kendall, M. G. and Stuart, A., The Advanced Theory of Statistics, Vol. III, Charles Griffin Co. Ltd., London,1966.

22. Kisiel, C. C., Time Series Analysis of Hydrologic Data in V. T. Chow (ed.), Advances in Hydroscience, Vol. 5, Academic Press, New York, 1969, pp.1-119.

23. Landsberg, H. E., Mitchell, J. M., and Crutcher, H. L., Power Spectrum Analysis of Climatological Data for Woodstock College, Maryland, Monthly Weather Review, Vol. 87, No. 8, 1959, pp.283-298.

24. Matalas, N. C., Autocorrelation of Rainfall and Stream-flow Minimums, U.S.G.S., Prof. Paper 434B, 1963.

25. McDonald, C. C. and Hughes, G. M., Studies of Consumptive Use of Water by Phreatophytes and Hydrophytes near Yuma, Arizona, U.S.G.S., Prof. Paper 486-F, 1968.

26. McDonald, J. E., Remarks on Correlation Methods in Geophysics, Tellus, XII, No. 2, 1960, pp.176-183.

27. Meinzer, O. E., Outline of groundwater hydrology with definition, U.S.G.S., Water Supply Paper 494, 1923.

28. Meyboom, P., Geology and Groundwater Resources of the Milk River Sandstone in Southern Alberta, Research Council of Alberta, Memoir 2, 1960.

29. Meyboom, P., Patterns of Groundwater Flow in the Prairie Profile in Groundwater, Proc. of Hydrology Symposium No. 3, The Queen's Printer, Ottawa, 1963.

30. Meyboom, P., Groundwater Studies in the Assiniboine River Drainage Basin, Part II Hydrologic Characteristics of Phreatophytic Vegetation in South Central Saskatchewan, Geological Survey of Canada, Bull. 139, 1967.

31. Panofsky, H. A., Meteorological Applications of Power Spectrum Analysis, Bulletin, American Meteorological Society, Vol. 36, No. 4, April 1955, pp.163-166.

32. Panofsky, H. A. and Brier, G. W., Some Applications of Statistics to Meteorology, Penn. State Univ., University Park, Pa., 1968.

33. Peck, A. J., The Water Table as Affected by Atmospheric Pressure, Journal of Geophysical Research, Vol. 65, No. 8, 1960.

34. Polowchak, Van M. and Panofsky, H. A., The Spectrum of Daily Temperature As A Climatic Indicator, Monthly Weather Review, Vol. 96, No. 9, 1968, pp.596-600.

35. Posey, J. W., The Weather and Circulation of September 1968, Monthly Weather Review, Vol. 96, No. 12, 1968, pp.893-898.

36. Quenouille, M. H., A large sample test for the goodness of fit of autoregressive schemes, Journal Royal Stat. Soc., Vol. 110, 1949, p.123.

37. Remson, I. and Randolph, J. R., Application of Statistical Methods to the Analysis of Groundwater Levels, Trans. A.G.U., Vol. 39, No. 1, 1958, pp.75-83.

38. Robinson, T. W., Phreatcphytes, U.S.G.S. Water Supply Paper 1423, 1958.

39. Sellers, W. D., Physical Climatology, The University of Chicago Press, Chicago, 1965.

40. Stark, L. P., The Weather and Circulation of August 1970, Monthly Weather Review, November 1970, pp.869-874.

41. Troxell, H. C., The Diurnal Fluctuation in the Groundwater and Flow of the Santa Ana River and its Meaning, Trans. A.G.U., 1936, pp.496-504.

42. White, W., A Method of Estimating Groundwater Supplies Based on Discharge by Plants and Evaporation from Soil, U.S.G.S., Water Supply Paper 659-A, 1932.

43. Yaglom, A. M., An introduction to the theory of stationary random functions, Prentice-Hall Inc., Englewood Cliffs, N.J., 1962.

44. Yu, S. L. and Brutsaert, W., Stochastic Aspects of Lake Ontario Evaporation, Water Resources Research, Vol. 5, No. 6, 1969, pp.1256-1266.

APPENDIX A

Observation Well Data

Well: K-1
Average water level, Summer 1967: 3.34 ft below datum
Description: 4-inch casing, gravel-packed, with a 5-foot long, 4-inch screen from 4 foot to 9 foot

Lithology:

Depth from	to	Lithology	Interpretation
0	9 feet	fine-grained sand	Alluvial
9	14	clayey silt	Alluvial
14	19	silty clay	Lacustrian
19	26	silty clay	Lacustrian
26		END OF HOLE	

Slug-test results: permeability: 2.85×10^{-3} cm/sec
induced phase lag: 6 minutes

Well: D-1
Average water level, Summer 1967: 3.94 ft below datum
Description: 4-inch casing slotted from 4.4 to 19.3 ft, gravel-packed

Lithology:

Depth from	to	Lithology	Interpretation
0	4 feet	clayey silt	Alluvial
4	7	silty clay	Alluvial
7	20	silty clay	Lacustrian
20		END OF HOLE	

Slug-test results: permeability: 3.84×10^{-4} cm/sec
induced phase lag: 21 minutes

APPENDIX B

```
C PROGRAM WHITE COMPUTES DAILY EVAPOTRANSPIRATION OF GROUNDWATER BY WHITE'S
C METHOD.  READ IN (N) SAMPLE SIZE,(SAMP) ALPHANUMERIC DATA ON THE HYDROGRAPH,
C (R)  GROUNDWATER INFLOW IN FT/HOUR, AND (S) DAILY DECLINE IN THE WATER LEVEL
C DUE TO EVAPOTRANSPIRATION FROM GROUNDWATER IN FT/DAY
C
      DIMENSION EVAP(200),R(200),S(200),SAMP(11)
      READ (1,1)  (SAMP(I),I=1,10),N,SY
      READ(1,2) (R(I),I=1,N)
      READ(1,2) (S(I),I=1,N)
      WRITE(3,99)  (SAMP(I),I=1,10),N,SY
C
C USE WHITE'S EQUATION TO CALCULATE EVAPOTRANSPIRATION
C
      DO 4 J=1,N
      FAC=(24.*R(J)+S(J))
    4 EVAP(J)=SY*FAC
C
C PRINT AND PUNCH OUT  VALUES OF DAILY EVAPOTRANSPIRATION
C
      WRITE(3,6)
      WRITE(3,7) (( J,R(J),S(J),EVAP(J)),J=1,N)
      WRITE(2,2) (EVAP(J),J=1,N)
      STOP
    1 FORMAT(10A4,I3,F4.2)
    2 FORMAT(16F5.3)
    6 FORMAT('1','          DAILY EVAPOTRANSPIRATION',//,'          DAY
     1    R      S     VALUE',//)
    7 FORMAT(11X,I2,2X,F6.3,1X,F5.3,3X,F5.3)
   99 FORMAT('1',10A4,' N=  ',I3, ' SY = ',F4.2,//)
      END
```

APPENDIX B

```
PROGRAM WHITE COMPUTES DAILY EVAPOTRANSPIRATION OF GROUNDWATER BY WHITE'S
METHOD.  READ IN (N) SAMPLE SIZE,(SAMP) ALPHANUMERIC DATA ON THE HYDROGRAPH,
(R)  GROUNDWATER INFLOW IN FT/HOUR, AND (S) DAILY DECLINE IN THE WATER LEVEL
DUE TO EVAPOTRANSPIRATION FROM GROUNDWATER IN FT/DAY

      DIMENSION EVAP(200),R(200),S(200),SAMP(11)
      READ (1,1)  (SAMP(I),I=1,10),N,SY
      READ(1,2) (R(I),I=1,N)
      READ(1,2) (S(I),I=1,N)
      WRITE(3,99)  (SAMP(I),I=1,10),N,SY

USE WHITE'S EQUATION TO CALCULATE EVAPOTRANSPIRATION

      DO 4 J=1,N
      FAC=(24.*R(J)+S(J))
    4 EVAP(J)=SY*FAC

PRINT AND PUNCH OUT  VALUES OF DAILY EVAPOTRANSPIRATION

      WRITE(3,6)
      WRITE(3,7) (( J,R(J),S(J),EVAP(J)),J=1,N)
      WRITE(2,2) (EVAP(J),J=1,N)
      STOP
    1 FORMAT(10A4, I3, F4.2)
    2 FORMAT(16F5.3)
    6 FORMAT('1','          DAILY EVAPOTRANSPIRATION',//,'          DAY
     1    R      S     VALUE',//)
    7 FORMAT(11X,I2,2X,F6.3,1X,F5.3,3X,F5.3)
   99 FORMAT('1',10A4,' N=  ',I3, ' SY = ',F4.2,//)
      END
```

APPENDIX C

Data List for Q,R,R, and T for 1968,1970,1971

Q = Groundwater evapotranspiration in ft/day

R = Groundwater inflow rate in ft/hour

P = Daily ppt in inches

T = Mean daily temperature in degrees Fahrenheit

DATA FOR YEAR 1968

DAY	Q	R	P	T
1	0.012	-.003	0.0	58.0
2	0.017	0.001	0.0	54.5
3	0.027	0.002	0.0	74.5
4	0.027	0.003	0.0	66.0
5	0.011	0.003	0.0	64.5
6	0.019	0.004	0.0	63.0
7	0.0	0.001	0.0	55.0
8	0.009	0.004	0.05	56.0
9	0.014	0.002	0.05	56.5
10	0.028	0.008	0.0	57.5
11	0.009	0.001	0.0	60.5
12	0.004	0.001	0.55	62.0
13	0.0	0.0	0.0	61.0
14	0.003	-.005	0.0	51.0
15	0.017	0.0	0.0	54.5
16	0.017	0.0	0.0	57.5
17	0.015	0.0	0.15	62.0
18	0.016	0.002	0.0	64.0
19	0.004	0.001	0.0	59.5
20	0.021	0.004	0.0	71.5
21	0.004	0.001	0.0	63.0
22	0.012	0.003	0.0	59.5
23	0.010	0.001	0.0	58.0
24	0.008	0.001	0.0	56.5
25	0.012	0.002	0.0	59.0
26	0.012	0.002	0.0	58.5
27	0.017	0.003	0.0	66.0
28	0.016	0.004	0.10	67.0
29	0.019	0.003	0.0	65.0
30	0.0	0.001	2.60	56.5
31	0.0	0.0	0.0	55.0
32	0.019	-.006	0.0	58.0
33	0.018	-.006	0.0	63.5
34	0.015	-.007	0.0	64.0
35	0.021	-.002	0.0	67.5
36	0.022	0.002	0.0	76.5
37	0.022	0.0	0.0	71.0
38	0.013	0.0	0.0	60.5
39	0.012	0.001	0.0	56.5
40	0.020	0.002	0.0	69.5
41	0.005	0.0	0.0	65.5
42	0.016	0.002	0.25	70.5
43	0.0	0.0	0.0	73.5
44	0.015	0.001	0.0	60.0

45	0.008	0.001	0.23	67.0
46	0.0	0.002	0.0	70.0
47	0.015	0.0	0.0	69.0
48	0.014	0.002	0.12	70.0
49	0.020	0.004	0.0	68.0
50	0.008	0.003	0.25	69.5
51	0.020	0.003	0.0	64.5
52	0.012	0.002	0.85	63.0
53	0.0	0.0	0.0	63.5
54	0.0	0.0	0.0	63.0
55	0.008	-.002	0.0	68.5
56	0.016	0.0	0.0	65.0
57	0.018	0.0	0.0	57.5
58	0.010	0.0	0.08	60.5
59	0.003	0.0	1.55	58.5
60	0.0	0.0	0.0	63.5
61	0.0	0.0	0.0	66.0
62	0.026	-.001	0.0	66.0
63	0.004	-.004	0.0	69.0
64	0.009	0.0	0.0	67.5
65	0.009	0.0	0.39	64.5
66	0.018	0.0	0.0	70.0
67	0.0	0.0	0.05	62.5
68	0.009	0.0	0.0	65.5
69	0.006	0.0	0.10	59.5
70	0.015	0.0	0.0	55.5
71	0.007	0.0	0.0	58.5
72	0.013	0.001	0.06	61.0
73	0.003	0.0	0.08	65.0
74	0.011	0.0	0.0	52.0
75	0.009	0.001	0.25	51.5
76	0.0	0.0	1.80	55.5
77	0.0	0.0	0.0	57.0
78	0.011	-.007	0.35	53.0
79	0.0	0.0	0.40	60.0
80	0.0	0.0	0.47	59.5
81	0.0	0.0	0.0	55.5
82	0.006	-.004	0.0	60.0
83	0.015	-.005	0.0	65.5
84	0.011	0.0	1.60	61.0
85	0.0	0.0	0.10	59.0
86	0.012	-.011	0.0	55.0
87	0.007	-.010	0.0	56.5
88	0.016	-.004	0.0	61.5
89	0.021	0.0	0.25	68.5
90	0.004	0.0	0.10	66.0
91	0.010	-.004	0.0	63.5
92	0.020	0.0	0.0	60.5
93	0.013	-.001	0.0	54.5
94	0.007	0.0	0.48	52.5
95	0.0	0.0	0.10	57.0

96	0.007	-.003	0.0	52.0
97	0.013	-.001	0.05	52.0
98	0.014	-.001	0.05	50.0
99	0.007	0.0	0.0	55.0
100	0.010	-.003	0.0	56.0
101	0.015	0.0	0.0	59.0
102	0.018	0.0	0.0	64.5
103	0.024	0.002	0.0	66.5
104	0.031	0.005	0.0	67.0
105	0.032	0.004	0.0	67.5
106	0.029	0.006	0.0	67.0
107	0.030	0.004	0.0	70.5
108	0.022	0.006	0.0	62.5
109	0.019	0.003	0.0	58.5
110	0.024	0.004	0.0	59.0
111	0.018	0.005	0.0	59.0
112	0.024	0.003	0.0	63.5
113	0.021	0.004	0.03	62.5

DATA FOR YEAR 1971

DAY	Q	R	P	T
1	0.0	0.0	0.34	67.0
2	0.001	-.006	0.02	62.0
3	0.013	-.003	0.0	65.0
4	0.004	-.005	0.0	57.0
5	0.0	-.002	0.33	56.5
6	0.0	0.0	0.0	60.0
7	0.005	-.002	0.04	59.0
8	0.002	-.002	0.09	62.0
9	0.007	0.0	0.0	57.0
10	0.003	-.001	0.0	53.0
11	0.003	-.002	0.0	61.5
12	0.003	0.0	0.13	66.0
13	0.004	0.0	0.02	60.0
14	0.004	-.001	0.15	59.0
15	0.003	-.001	0.29	62.0
16	0.0	0.0	0.35	57.5
17	0.0	0.0	0.0	58.5
18	0.003	-.002	0.17	60.5
19	0.001	-.002	0.06	65.0
20	0.005	0.0	0.0	57.0
21	0.004	-.002	0.0	61.0
22	0.0	-.003	0.23	61.0
23	0.006	0.0	0.0	63.0
24	0.003	-.003	0.0	58.5
25	0.004	0.0	0.74	51.0
26	0.0	0.0	0.02	58.0
27	0.0	0.0	0.07	61.5
28	0.006	0.0	0.05	65.0
29	0.004	-.003	0.0	63.5
30	0.008	-.001	0.0	60.5
31	0.009	-.001	0.46	65.0
32	0.004	0.0	0.0	55.0
33	0.003	0.0	0.20	54.0
34	0.005	0.0	0.0	61.0
35	0.004	0.0	0.01	60.0
36	0.004	0.0	0.0	60.5
37	0.002	-.003	0.0	56.5
38	0.007	0.0	0.0	57.5
39	0.003	0.0	0.14	57.5
40	0.012	0.004	0.0	70.5
41	0.005	0.0	0.43	54.0
42	0.005	0.002	0.01	54.0
43	0.0	0.0	0.37	51.0
44	0.0	0.0	0.24	49.5

45	0.0	0.0	0.0	52.0
46	0.0	0.0	0.0	57.0
47	0.002	0.0	0.0	59.0
48	0.006	-0.001	0.0	56.0
49	0.005	-0.001	0.0	49.5
50	0.007	-0.001	0.0	53.0
51	0.010	-0.001	0.0	55.5
52	0.006	-0.001	0.0	64.0
53	0.007	0.0	0.0	64.0
54	0.007	0.0	0.0	67.5
55	0.007	0.0	0.0	71.0
56	0.007	0.0	0.0	67.5
57	0.002	-0.001	0.06	58.5
58	0.004	0.0	0.0	62.0
59	0.008	0.0	0.0	56.0
60	0.003	0.0	0.04	51.5
61	0.004	0.0	0.0	59.5
62	0.007	0.0	0.01	77.0
63	0.003	0.0	0.04	69.0
64	0.006	0.001	0.0	69.5
65	0.005	0.0	0.0	61.0
66	0.001	0.0	0.43	61.5
67	0.008	0.003	0.0	64.0
68	0.009	0.003	0.0	66.5
69	0.006	0.0	0.0	65.0
70	0.005	0.0	0.03	63.5
71	0.007	0.002	0.0	57.0
72	0.002	0.0	0.0	59.0
73	0.004	0.0	0.0	64.0
74	0.006	0.0	0.0	69.5
75	0.003	0.0	0.0	72.0
76	0.006	0.0	0.0	64.5
77	0.003	0.0	0.0	60.0
78	0.001	0.0	0.0	53.0
79	0.0	0.0	0.04	60.0
80	0.009	0.002	0.0	59.5
81	0.002	0.0	0.03	65.5

DATA FOR YEAR 1970

DAY	Q	R	P	T
1	0.020	-.002	0.10	66.0
2	0.0	0.0	0.04	56.5
3	0.043	0.0	0.0	51.0
4	0.007	0.0	0.0	50.5
5	0.014	-.003	0.0	59.0
6	0.017	-.001	0.0	62.5
7	0.015	0.0	0.0	66.5
8	0.003	0.0	0.14	63.5
9	0.005	-.002	0.0	55.5
10	0.0	0.0	0.22	58.5
11	0.011	-.003	0.0	61.5
12	0.008	0.0	0.06	68.0
13	0.014	0.0	0.0	76.0
14	0.006	-.003	0.0	71.5
15	0.018	0.004	0.11	74.0
16	0.010	0.0	0.0	63.5
17	0.009	0.0	0.03	61.0
18	0.0	-.002	0.01	54.0
19	0.004	0.0	0.0	57.5
20	0.006	0.0	0.0	65.5
21	0.007	0.0	0.10	69.5
22	0.014	0.002	0.0	63.5
23	0.008	0.001	0.0	65.0
24	0.008	0.001	0.0	68.0
25	0.012	0.002	0.0	69.5
26	0.006	0.001	0.0	74.0
27	0.012	0.004	0.18	71.5
28	0.005	0.002	0.07	67.5
29	0.0	0.0	2.96	63.0
30	0.008	0.0	0.0	65.0
31	0.024	-.005	0.0	69.5
32	0.014	-.010	0.0	65.5
33	0.005	-.003	0.01	58.0
34	0.018	-.006	0.0	57.5
35	0.027	-.001	0.0	57.0
36	0.018	0.0	0.0	63.5
37	0.012	0.0	0.01	64.5
38	0.002	0.0	1.10	60.0
39	0.020	-.006	0.0	63.5
40	0.015	-.008	0.0	66.0
41	0.024	-.007	0.0	69.5
42	0.015	-.003	0.0	63.0
43	0.016	0.0	0.0	69.0
44	0.012	0.0	0.0	72.5

45	0.012	-.001	0.0	71.5
46	0.005	-.003	0.0	62.5
47	0.014	0.0	0.0	66.5
48	0.008	-.002	0.0	59.0
49	0.005	-.001	0.0	57.0
50	0.011	0.0	0.0	64.0
51	0.010	0.0	0.0	65.5
52	0.009	0.0	0.0	68.5
53	0.012	0.001	0.0	76.5
54	0.013	0.001	0.0	70.5
55	0.014	0.001	0.0	65.0
56	0.010	0.001	0.0	69.0
57	0.009	0.001	0.02	69.0
58	0.012	0.002	0.0	67.5
59	0.011	0.002	0.0	74.0
60	0.004	-.002	0.0	67.5
61	0.011	0.004	0.23	59.0
62	0.004	-0.001	0.0	56.5
63	0.020	0.006	0.0	67.5
64	0.008	0.0	0.0	66.0
65	0.005	0.0	0.0	55.0
66	0.006	0.001	0.0	51.0
67	0.012	0.005	0.0	52.5
68	0.007	0.001	0.0	56.5
69	0.015	0.004	0.0	58.0
70	0.015	0.005	0.0	58.0
71	0.005	0.0	0.0	56.5
72	0.011	0.004	0.0	58.5
73	0.004	-.001	0.0	55.0
74	0.009	0.003	0.0	51.0
75	0.009	0.004	1.13	60.5
76	0.0	0.0	0.0	52.5
77	0.0	0.0	0.0	51.0
78	0.0	0.0	0.0	62.0
79	0.0	0.0	0.01	65.5
80	0.005	0.002	0.0	61.5
81	0.003	0.001	0.0	57.5
82	0.008	0.003	0.0	71.5
83	0.007	0.0	0.0	69.0
84	0.004	0.0	0.06	52.0
85	0.003	0.001	0.02	51.5
86	0.012	0.003	0.01	46.0
87	0.010	0.003	0.0	40.5

APPENDIX D

```
C  PROGRAM SPECTRA
C
C     SPECTRAL ANALYSIS AND FILTERING
C  VERSION OF R.E. JACKSON FOR HYDROLOGICAL AND CLIMATOLOGICAL DATA ANALYSIS
C
C
C
C.....EXPLANATION AND ORDER OF INPUT.....
C
C FIRST CARD -  COLUMNS -  NAME  -  COMMENTS
C
C                 1-40      SAMP(J)   ANY ALPHANUMERIC INFORMATION
C                41-43      ID        SAMPLE NO., MUST BE DIFFERENT FROM ZERO
C                44-46      M         MAXIMUM LAG, MUST NOT EXCEED 50
C                47-49      ILG       CODE AS TO WHETHER WE USE RAW DATA OR LOG
C                                     TRANSFORMED DATA.IF ILG=1 WE USE THE LOG
C                                     TRANSFORM,OTHERWISE THE RAW DATA IS USED
C                50-52      N         NUMBER OF DATA POINTS
C
C  SAMPLE NUMBERS 1-10 ARE RESERVED FOR GROUNDWATER EVAPOTRANSPIRATION (Q) AND
C  INFLOW RATE (R) IN FORMAT 16F5.3.
C  SAMPLE NOS. 11-15  ARE FOR DAILY PPT (P) IN FORMAT 20F4.2
C  SAMPLE NOS. 16-20 ARE FOR DAILY MEAN TEMP(T) IN FORMAT 20F4.1
C  EQUATION NUMBERS REFER TO EQUATIONS IN THE THESIS
C ONE BLANK CARD AFTER LAST DATA DECK
C
C NOTE IF LOG OPTION IS REQUIRED, THE LOGGING OF THE DATA SHOULD BE DONE IN DO
C  LOOP 401, I.E. CARD SPEC 205
C
C
C  NOTE --- CARD OUTPUT CONSISTS OF STANDARDIZED DATA AND FITTED SIGNAL VALUE
C
C
C
C
C
C
C
C
C
C
```

```
      DIMENSION X(200),VC(50),C(50)
      COMMON R(50),XX(200),SAMP(10),IN,IOUT,V(50),LH,QC,SUD(50),H(50)
      PIE=3.14159265
      IOUT=3
      IN=1
C-----------------------------------------------------------------------
C  READ IN FIRST CARD
C-----------------------------------------------------------------------
   50 READ(IN,1)(SAMP(J),J=1,10),ID,M,ILG,N
      IF(ID)100,999,100
  100 WRITE(IOUT,2)(SAMP(J),J=1,10),ID,M
      IF (ILG.EQ.10) GO TO 110
      GO TO 120
  110 WRITE(IOUT,3)
      GO TO 130
  120 WRITE(IOUT,4)
  130 XM=M
      PDE=PIE/XM
      I = 1
      SUM2=0.0
      SUM=0.0
C-----------------------------------------------------------------------
C  READ IN DATA DECK
C-----------------------------------------------------------------------
      IF (ID.LE.10)  READ(IN,400) (X(I),I=1,N)
      IF(ID.GE.11).AND. ID.LE.15) READ(IN,399)  (X(I),I=1,N)
      IF(ID.GT.15)  READ(IN,398)  (X(I),I=1,N)
      WRITE(IOUT,20) (SAMP(J),J=1,10)
      WRITE(IOUT,397)  (X(I),I=1,N)
      DO 401 J=1,N
  401 SUM=SUM+X(J)
      XI=N
      I=N
C-----------------------------------------------------------------------
C  COMPUTE STATISTICS OF TIME SERIES AND FORM STANDARDISED TIME SERIES
C-----------------------------------------------------------------------
      XBAR = SUM / XI
      DO 190 J=1,I
      X(J)=X(J)-XBAR
  190 SUM2=SUM2+(X(J)**2)
      VAR = SUM2 / (XI - 1.0)
      SD=SQRT (VAR)
      SUM3=0.0
      DO 191 J=1,N
      X(J)=X(J)/SD
  191 SUM3=SUM3+X(J)**2
      CO=SUM3/XI
C-----------------------------------------------------------------------
```

```
C  COMPUTE ACVF
C-----------------------------------------------------------------
      MM1=M-1
      DO 210 L=1,M
      JX=I-L
      XSUM=0.0
      DO 200 JK=1,JX
      JY=JK+L
  200 XSUM=XSUM+X(JK)*X(JY)
      XJ = JX
      C(L) = (1.0 / XJ) * XSUM
  210 R(L)=C(L)/CC
C-----------------------------------------------------------------
C  ESTIMATE SPECTRUM
C-----------------------------------------------------------------
      DO 230 L=1,M
      XL = L
      SUMYC=0.0
      SUMY=0.0
      DO 220 J=1,MM1
      XJ = J
      ARG1 = COS (XL * XJ * PDE)
      ARG2=C(M)*COS (XL*PIE)
      SUMY = SUMY + C(J) * ARG1
  220 SUMYC = SUMYC + C(J) * ARG1 * (1.0 + COS (XJ * PDE))
      V(L) = CO  +  2.0 * SUMY + ARG2
  230 VC(L) = CO + SUMYC
      CJ = 0.0
      CJJ=0.0
      DO 240 JJ=1,MM1
      XJJ=JJ
      CJJ=CJJ + C(JJ)*(1.0+COS (XJJ*PDE))
  240 CJ = CJ + C(JJ)
      VO=CO +2.0*CJ +C(M)
      VOH = CO+CJJ
C-----------------------------------------------------------------
C  CALL SUBROUTINE TO COMPUTE THEORETICAL ACVF AND SPECTRUM
C-----------------------------------------------------------------
      PHC1=R(1)
      CALL MARKOV(RHO1,CO,PIE,M,HZERO,CHISUM,N)
      WRITE(IOUT,7)I,XBAR,VAR,SD
      WRITE(IOUT,20)(SAMP(J),J=1,10)
      WRITE(IOUT,6)CO,VO,VOH,HZERO
      WRITE(IOUT,8)
      DO 250 J=1,M
  250 WRITE(IOUT,9)J,R(J),C(J),V(J),VC(J),RHO(J),H(J)
      WRITE(IOUT,256) CHISUM
      IF(ID.GE.11)  GO TO 50
      DO 260 JJ=1,I
  260 XX(JJ)=X(JJ)
      WRITE(IOUT,20)(SAMP(J),J=1,10)
```

```
C-----------------------------------------------------------------
C  PRINT AND PUNCH OUT STANDARDISED DATA
C-----------------------------------------------------------------
      WRITE(IOUT,12)
      DO 290 J=1,I
  290 WRITE(IOUT,13)J,X(J)
C-----------------------------------------------------------------
C  CALL SUBROUTINE FILTER
C-----------------------------------------------------------------
      CALL FILTER(N,I,VAR,DUM)
      IF(DUM.LT.0.0)  GO TO 50
      WRITE(IOUT,20)(SAMP(J),J=1,10)
C-----------------------------------------------------------------
C  PRINT AND PUNCH OUT THE SIGNAL
C-----------------------------------------------------------------
      WRITE(IOUT,14)LH,LH
      LH1=LH+1
      LH2=I-LH
      DO 320 J=LH1,LH2
      SUM=QQ*X(J)
      IF(LH.EQ.0) GO TO 320
      GO TO 300
  300 DO 310 JJ=1,LH
      JJ1=J+JJ
      JJ2=J-JJ
  310 SUM=SUM+XX(JJ)*(X(JJ1)+X(JJ2))
  320 WRITE(IOUT,15)J,SUM
      GO TO 50
  999 STOP
    1 FORMAT(10A4,4I3)
    2 FORMAT(1H1,10A4//1H ,12HSAMPLE NO.= ,I3//1H ,13HMAXIMUM LAG= ,I
    3 FORMAT(//30X,30H..........LOG OPTION..........)
    4 FORMAT(//30X,40H..........LOG OPTION NOT TAKEN..........)
    5 FORMAT(8X,I3,48X,F8.3 )
    6 FORMAT(////1H ,7HC ZERO=, F12.5, 12X, 7HV ZERO=, F12.5,12X,16H=
     CED V ZERO=, F12.5,12X,20HTHEORETICAL V ZERO= ,F12.5/)
    7 FORMAT(///1H ,16HNO. OF SAMPLES =,I5//1H ,6HMEAN =,F12.5//1H ,
     CARIANCE =,F12.5//1H ,15HSTANDARD DEVN.=,F12.5 )
    8 FORMAT(///1H ,1X,3HLAG,2X,15HAUTOCORRELATION,2X,14HAUTOCOVARIA
     12X,16HSPECTRAL DENSITY,3X,15HWARNED SPECTRUM,1X,14HTHEO. SPE,5
     323HTHEO. SPECTRAL DENSITY//1H ,2X,2HL ,8X,4HR(L),10X,4HCV(L),
     412X,4HV(L),11X,11HWARNED V(L),6X,6HRHO(L),12X,4HH(L)//)
    9 FORMAT(1H ,I2,4X,F10.7,3(5X,F13.7),3X,F10.7,5X,E13.7)
   10 FORMAT(///1H ,88HRELATIVE VARIANCE TIMES VOLUME= LAG*(VAR AT L
     CALUE)/(VAR AT LAG 1).COMPUTED FROM DATA//1H ,2X,3HLAG,5X,5HVALU
   11 FORMAT(1H ,I3,2X,F12.5)
   12 FORMAT(///1H ,29HPRINTOUT OF STANDARDISED DATA//1H ,1X,3HLAG,8X,
     C5HVALUE/)
   13 FORMAT(1H ,I3,5X,F10.4)
   14 FORMAT(////40H SIGNAL VALUES COMPUTED BY SUMMING FROM LAG= ,I3,
     C,7HTO LAG=,I3//1H ,10HSAMPLE NO.,7X,12HSIGNAL VALUE )
```

```
   15 FORMAT(1H ,3X,I4,6X,F12.6)
   20 FORMAT(1H1,10A4)
   21 FORMAT(50X,F8.4)
   22 FORMAT(9X,I3,48X,F8.4 )
  396 FORMAT(////1H ,'          SUM OF CHI SQUARES    = ',F10.5)
  397 FORMAT(10X,10F8.3)
  398 FORMAT(20F4.1)
  399 FORMAT(20F4.2)
  400 FORMAT(16F5.3)
      END


      SUBROUTINE FILTER(M,N,VAR,DUM)
      DIMENSION RL (50),VV(200),RC(50),T(50),Y(50)
      COMMON R(50),XX(200),SAMP(10),IN,IOUT,V(53),LH,QQ,PHO(50),H(50)
C-----------------------------------------------------------------------
C  CARRIES OUT FILTERING OPERATION
C-----------------------------------------------------------------------
      EQUIVALENCE (VV(1),XX(1)),(RL(1),V(1)),(RC(1),V(11))
      WRITE(IOUT,1)(SAMP(I),I=1,10)
  100 I=1
  110 IF(R(I))130,130,120
  120 I=I+1
      IF(I- M)110,130,130
C-----------------------------------------------------------------------
C  CALCULATE A AND C BY SIMPLE LINEAR REGRESSION (EQNS. 2.21 AND 2.22)
C-----------------------------------------------------------------------
  130 IT=I-1
      DO 131 J=1,IT
      Y(J)=ALOG(R(J))
  131 T(J)=J
      A=0.0
      B=0.0
      C=0.0
      D=0.0
      E=0.0
      DO 132 J=1,IT
      A=A+(T(J)*Y(J))
      B=B+T(J)
      C=C+Y(J)
      D=D+T(J)**2
  132 E=E+Y(J)**2
      TM=B/IT
      YM=C/IT
      AA=(A-IT*TM*YM)/(D-IT*TM**2)
      CC=EXP(YM-AA*TM)
      WRITE(IOUT,2)
      WRITE(IOUT,3)CC,AA
      WRITE(IOUT,2)
      DO 150 J=1,M
```

```
      WRITE(IOUT,4)
      XJ=J
      RL(J)=CC*EXP (AA*XJ)
  150 WRITE(IOUT,5)J,R(J),RL(J)
C
C  CALCULATE P AND Q (EQN.2.26)
C
      AA=-AA
      DUM =(AA**2+2.0*(AA*CC/(1.0-CC)))
      IF (DUM.LT.0.0)  WRITE(IOUT,15)
      IF (DUM.LT.0.0) GO TO 211
      PP=SQRT(DUM)
      QQ=AA*CC/(PP*(1.-CC))
      WRITE(IOUT,9)QQ,PP
      EXSM=EXP (-PP)
C-----------------------------------------------------------------
C  CALCULATE H=SML (EQN.2.30)
C-----------------------------------------------------------------
      SML=QQ+2.*QQ*(EXSM/(1.-EXSM))
      WRITE(IOUT,10)SML
      WRITE(IOUT,11)
      WRITE(IOUT,12)QQ,QQ
      HSM=QQ
      J=0
C-----------------------------------------------------------------
C  CHECK THAT EQN.2.28 IS SATISFIED
C-----------------------------------------------------------------
      IF((SML-HSM)-.05)200,180,180
  180 DO 190 J=1,50
      XJ=J
      VV(J)=QQ*EXP (-(XJ*PP))
      HSM=HSM+2.*VV(J)
      WRITE(IOUT,13)J,VV(J),HSM
      IF((SML-HSM)-.05)200,190,190
  190 CONTINUE
  200 LH=J
C-----------------------------------------------------------------
C  CALCULATE CORRECTED FILTER (EQN.2.31)
C-----------------------------------------------------------------
      WRITE(IOUT,14)
      CORF=SML/HSM
      QQ=CORF*QQ
      WRITE(IOUT,11)
      WRITE(IOUT,12)QQ,QQ
      SUM=QQ
      DO 210 J=1,LH
      VV(J)=CORF*VV(J)
      SUM=SUM+VV(J)*2.
  210 WRITE(IOUT,13)J,VV(J),SUM
  211 RETURN
    1 FORMAT(1H1,10A4)
```

```
    2 FORMAT(1H0)
    3 FORMAT(1H0,44H DERIVED FORMULA FOR AUTOCORRELATION FUNCTION //
     C,7H R(L) =,F10.7,6H*EXP (,E13.6,4H * L ))
    4 FORMAT(///3X,24HAUTOCORRELATION,COMPUTED/1H ,1X,5HLAG  ,2X,15H(1
     FROM SAMPLE ,2X,16H(2)FROM EQUATION / )
    5 FORMAT(1H ,I3,2(5X,F13.7))
    6 FORMAT(///1H ,99HRELATIVE VARIANCE TIMES VOLUME= LAG*(VAR AT LAG
     1ALUE)/(VAR AT LAG 1).COMPUTED FROM DERIVED EQN.//4X,3HLAG,5X,9HV
     2UE/)
    7 FORMAT(1H ,I5,3X,E10.5)
    8 FORMAT(///1H ,32HSTANDARD DEVIATION OF THE MEAN= ,F12.7 )
    9 FORMAT(///1H ,15HFILTER H(L) = (,F10.7,14H)*EXP(-ABS(L)*,E12.7,1
     C )
   10 FORMAT(///1H ,34HSUM OF H(L) OVER ALL LAG VALUES = ,F12.7 )
   11 FORMAT(///1H ,20X,20HSUM FROM -LAG TO LAG )
   12 FORMAT(//1H ,8HH( 0 ) =,F10.7,6X,E13.7)
   13 FORMAT(1H ,2HH(,I3,3H) =,F10.7,6X,E13.7 )
   14 FORMAT(///1H ,32HCORRECTED FILTER VALUES AND SUMS )
   15 FORMAT('1','    NO FILTER POSSIBLE - DUM  LT. 0.0')
      END


      SUBROUTINE MARKOV(RHO1,VAR,PIE,M,NZERO,CHISUM,N)
      COMMON R(50),XX(200),SAMP(10),IN,IOUT,V(50),LH,QQ,RHO(50),H(50)
      DIMENSION CHI(50)
C-----------------------------------------------------------------
C  COMPUTES THEORETICAL SPECTRUM AND CORRELOGRAM OF FIRST
C  ORDER MARKOV PROCESS
C-----------------------------------------------------------------
      IF(RHO1.LT.0.0) GO TO 2
C
C  RHO1 IS POSITIVE
C
      DO 1 I=1,M
      A=I
      RHO(I)=RHO1**A
      D=2.*PIE*A/(2.*M)
    1 P(I)=VAR*(1.-RHO1**2.)/(1.+RHO1**2.-2.*RHO1*COS(D))
      CHI(1)=(N-K)*(P(1)-2.*R(1)+(P(1)**3))**2/(1.-R(1)**2)**2
      CHI(2)=(N-K)*(P(2)-R(1)**2)**2/(1.-R(1)**2)**2
      DO 5 K=3,M
      K1=K-1
      K2=K-2
      PK=P(K)-2.*R(1)*R(K1)+(R(1)**2)*R(K2)
    5 CHI(K)=((N-K)*PK**2)/(1.-P(1)**2)**2
      CHISUM=0.0
      DO 6 K=1,M
    6 CHISUM=CHISUM+CHI(K)
      GO TO 4
C
```

```
C  RHO1 IS NEGATIVE
C
      2 RHO1=ABS(RHO1)
        B=1.
        DO 3 I=1,M
        B=-B
        A=I
        RHO(I)=B*RHO1**A
        D=2.*PI**A/(2.**N)
      3 H(I)=VAR*(1.-RHO1**2.)/(1.+RHO1**2+2.*RHO1*COS(D))
        CHI(1)=(N-K)*(RHO1-2.*RHO1-RHO1**3)**2/(1.-RHO1**2)**2
        CHI(2)=(N-K)*(RHO1-2.*RHO1**2+RHO1**2)**2/(1.-RHO1**2)**2
        DO 7 K=3,M
        K1=K-1
        K2=K-2
        RK=R(K)-2.*R(1)*R(K1)+(RHO1**2)*R(K2)
      7 CHI(K)=((N-K)*RK**2)/(1.-RHO1**2)**2
        CHISUM=0.0
        DO 8 K=1,M
      8 CHISUM=CHISUM+CHI(K)
C
      4 HZERO=VAR*(1.+RHO1)/(1.-RHO1)
        RETURN
        END
```